Swarm Precise Orbit Determination

Adrian Jäggi

AIUB

Astronomical Institute
University of Bern

Low Earth Orbiters (LEOs)

CHAMP

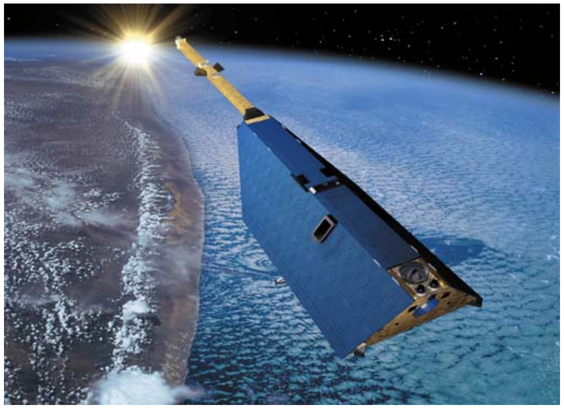

CHAllenging **M**inisatellite **P**ayload

GRACE

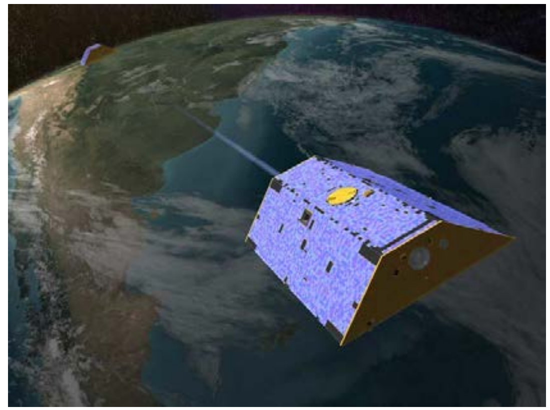

Gravity **R**ecovery **A**nd **C**limate **E**xperiment

GOCE

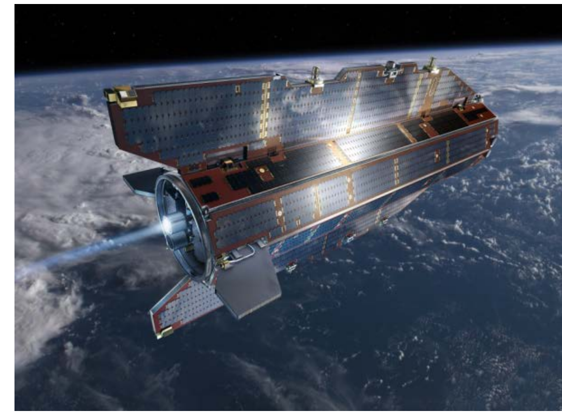

Gravity and steady-state **O**cean **C**irculation **E**xplorer

But there are many more missions equipped with GPS receivers …

Jason

Jason-2

MetOp-A

Icesat

COSMIC

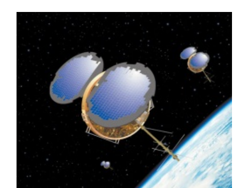

LEO Constellations

TanDEM-X

Swarm

Sentinel

and of course, in the future

Global Navigation Satellite Systems (GNSS)

GPS

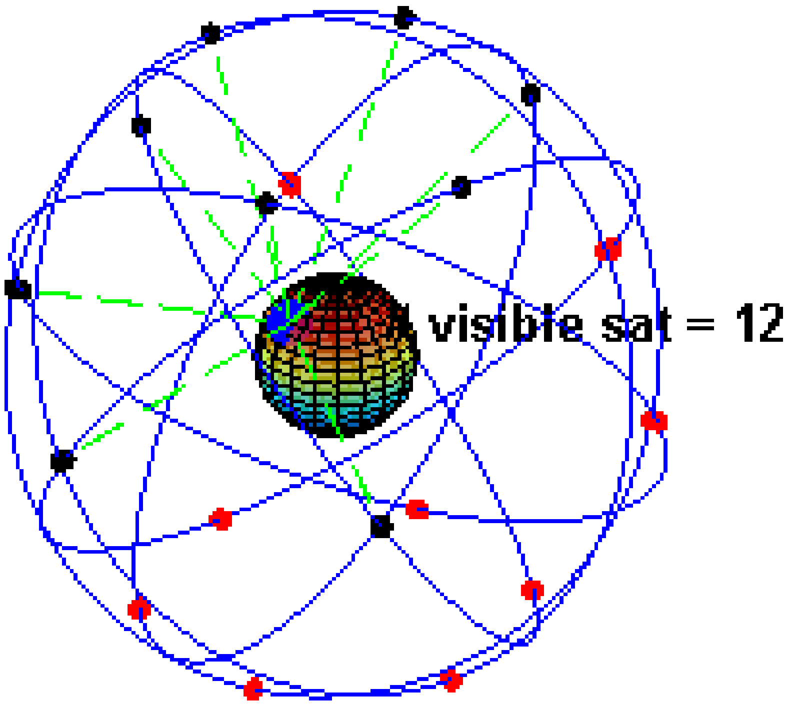

Galileo

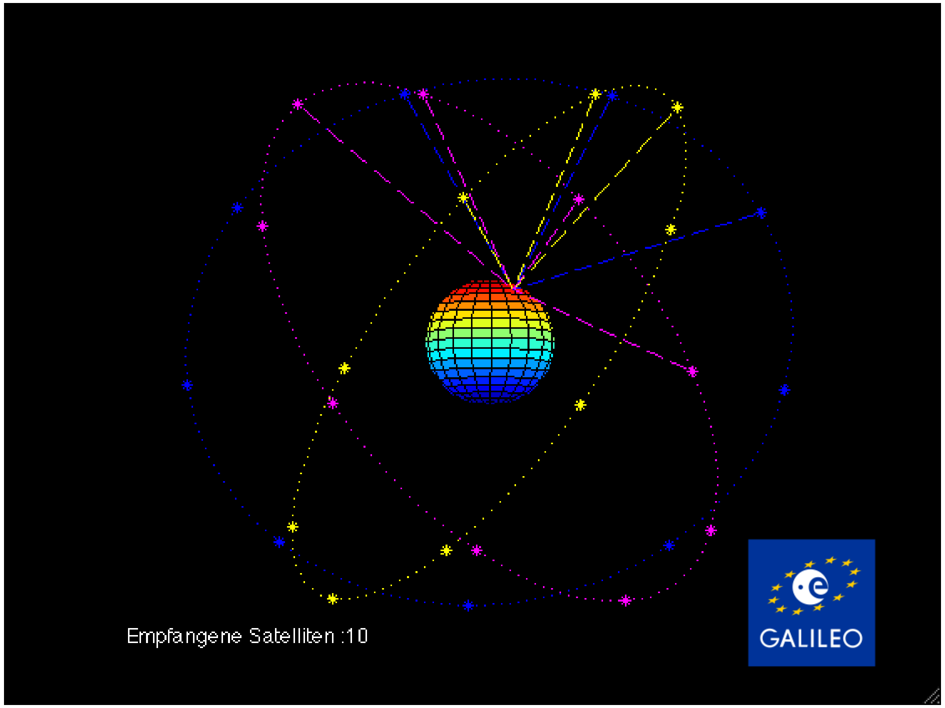

Other GNSS are already existing (GLONASS) or being built up (Galileo, Beidou), but there are no multi-GNSS spaceborne receivers (with open data policy) in LEO orbit yet.

Introduction to GPS

GPS: **G**lobal **P**ositioning **S**ystem

Characteristics:

- Satellite system for (real-time) **Positioning** and **Navigation**
- **Global** (everywhere on Earth, up to altitudes of 5000km) and **at any time**
- **Unlimited** number of users
- **Weather-independent** (radio signals are passing through the atmosphere)
- **3-dimensional position**, **velocity** and **time** information

Global Network of the International GNSS Service (IGS)

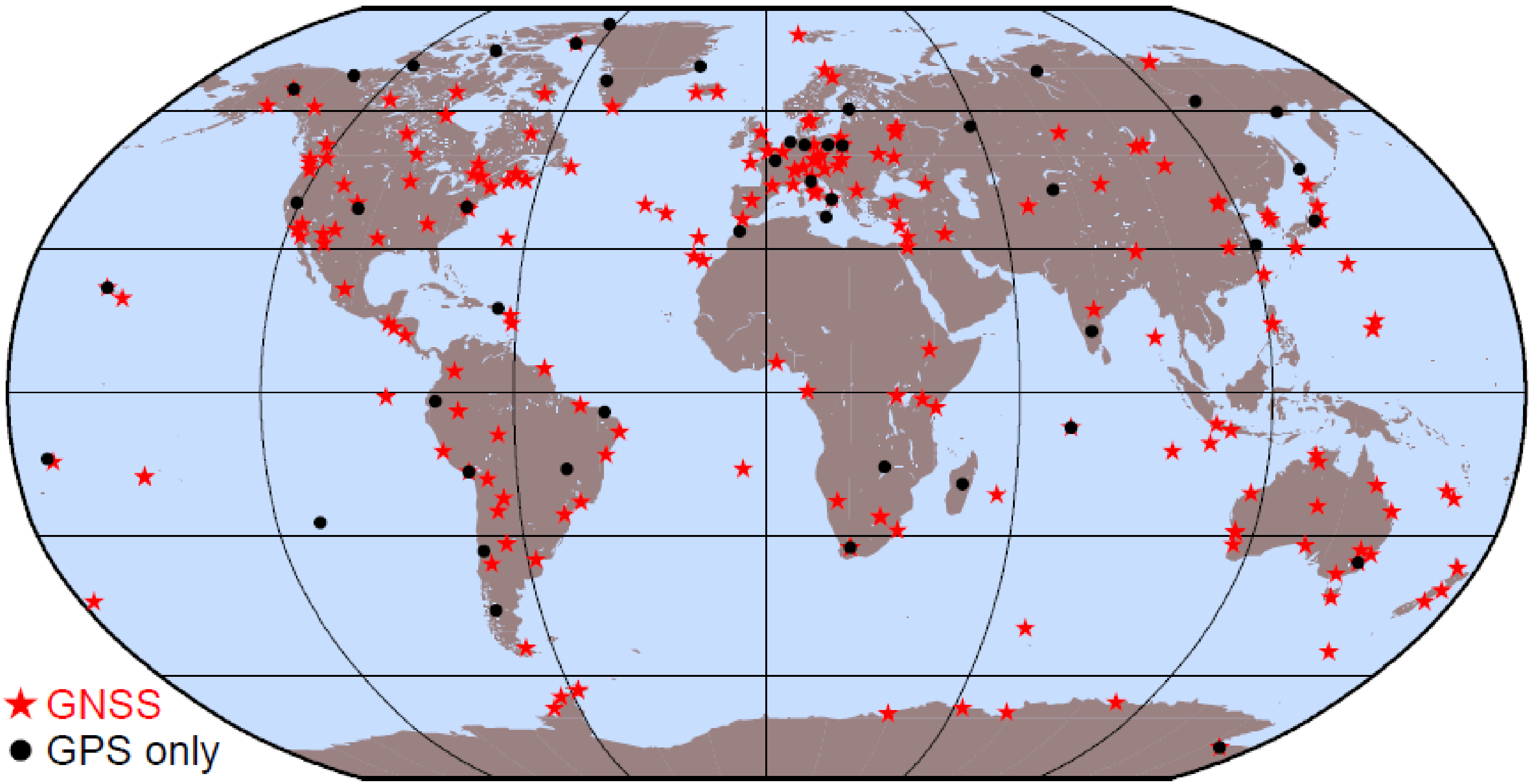

IGS stations used for computation of final orbits at CODE in June 2016 (Dach et al., 2009)

Parameters of a Global IGS Solution

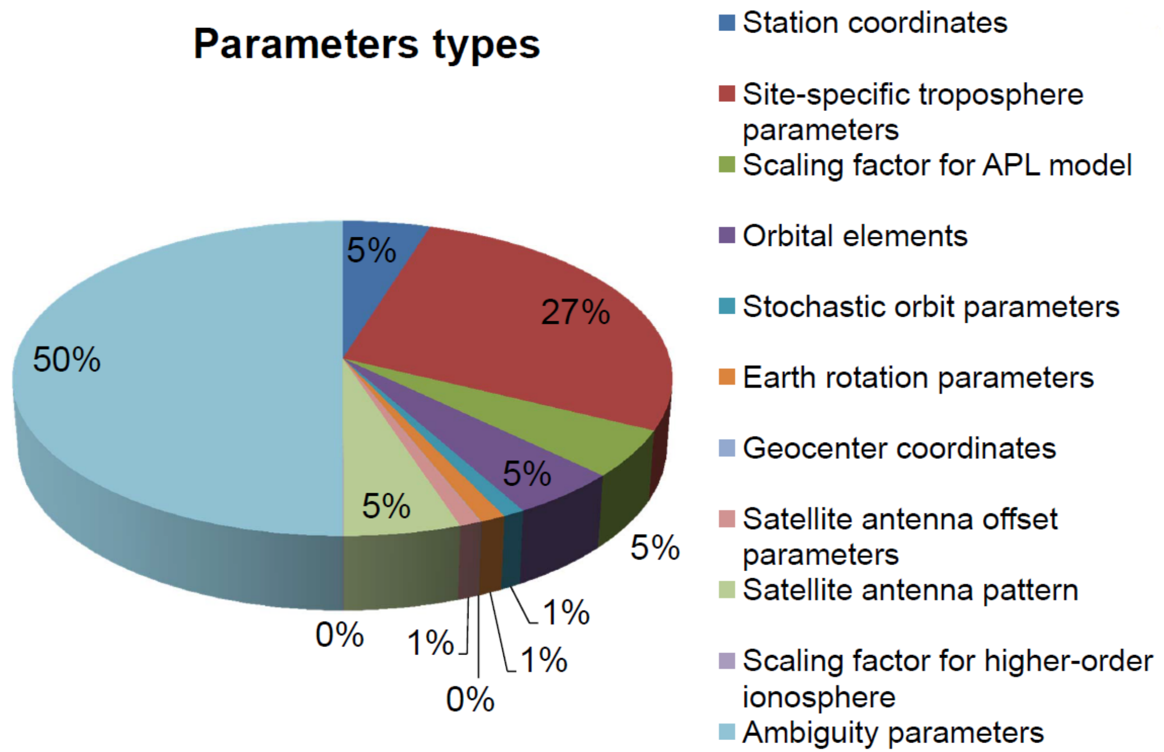

- A large parameter estimation problem needs to be solved to determine GPS satellite orbits together with many other parameters on a routine basis
- Thanks to this continuous effort performed by the Analysis Centers (ACs) of the **International GNSS Service (IGS)** many scientific applications are enabled

Performance of IGS Final Orbits

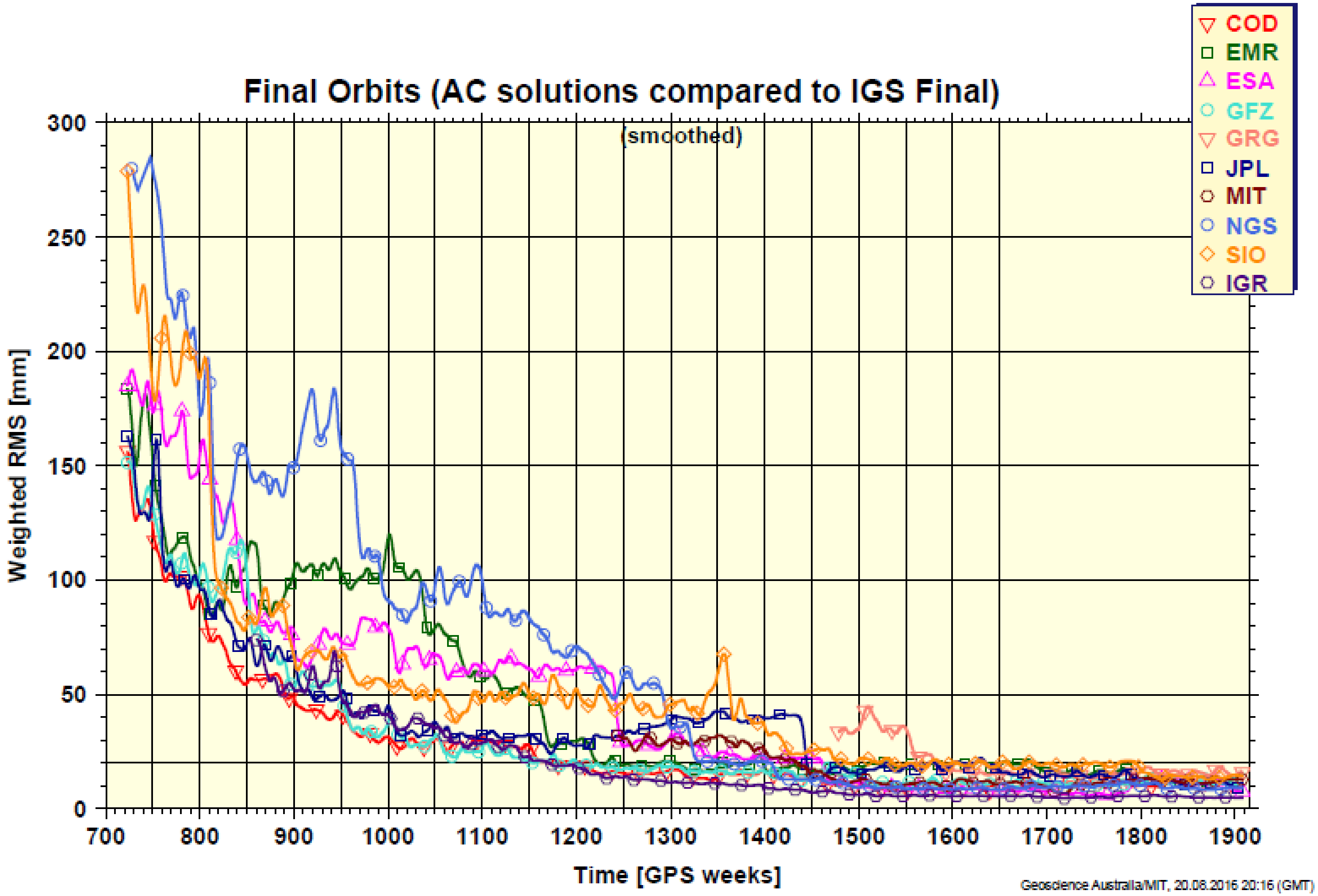

Computation of GNSS Clock Corrections

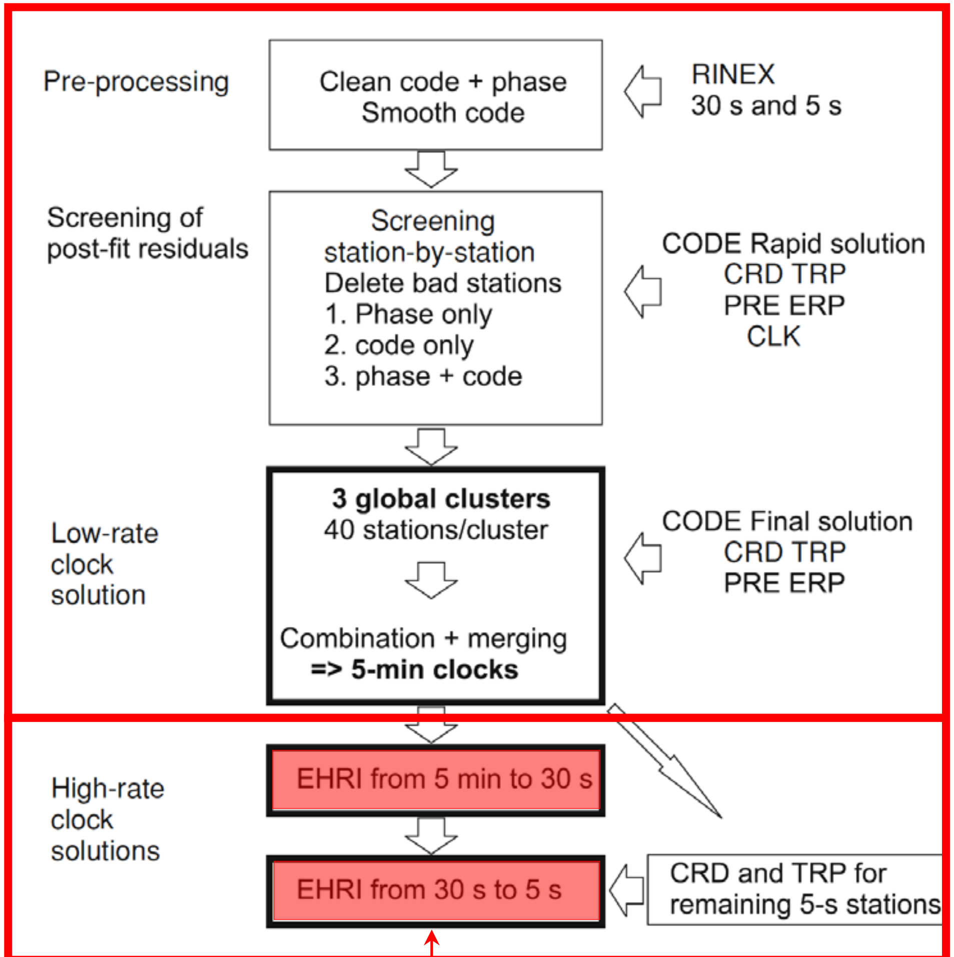

(Bock et al., 2009)

The final clock product with 5 min sampling is based on undifferenced GPS data of typically 120 stations of the IGS network

The IGS 1 Hz network is finally used for clock densification to 5 sec

The 5 sec clocks are interpolated to 1 sec as needed for 1 Hz LEO GPS data

GPS Signals

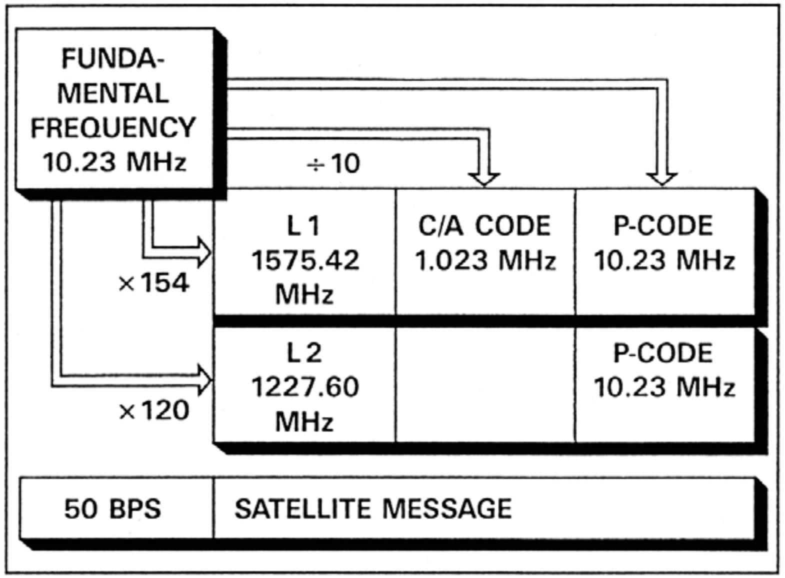

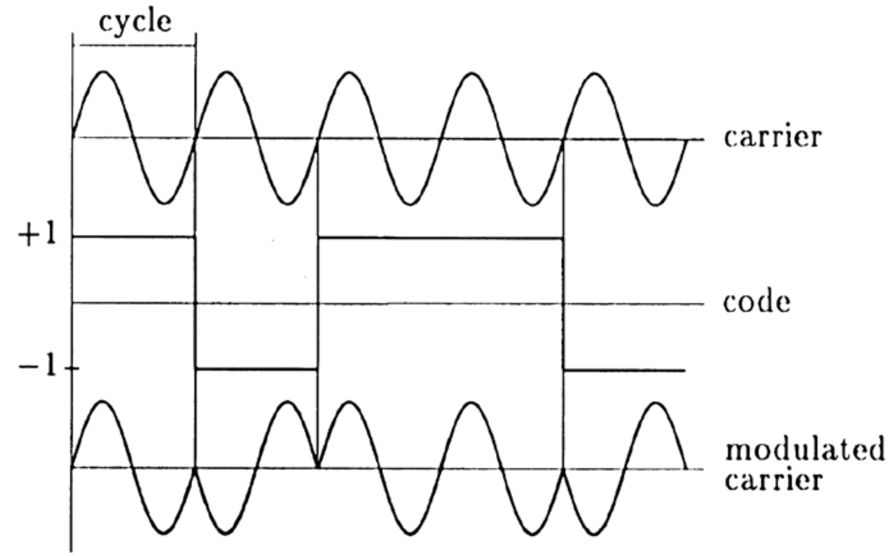

Signals driven by an **atomic clock**

Two **carrier signals** (sine waves):

- **L_1**: f = 1575.43 MHz, λ = 19 cm
- **L_2**: f = 1227.60 MHz, λ = 24 cm

Bits encoded on carrier by phase modulation:

- **C/A-code** (Clear Access / Coarse Acquisition)
- **P-code** (Protected / Precise)
- **Broadcast/Navigation Message**

(e.g. Blewitt, 1997)

Improved Observation Equation

$$L_i^k = \rho_i^k - c \cdot \Delta t^k + c \cdot \Delta t_i + \cancel{T_i^k} + \cancel{I_i^k} + \lambda \cdot N_i^k$$
$$+ \Delta_{rel} - c \cdot b^k + c \cdot b_i + m_i^k + \epsilon_i^k$$

ρ_i^k	Distance between satellite and receiver
Δt^k	Satellite clock offset wrt GPS time
Δt_i	Receiver clock offset wrt GPS time
~~T_i^k~~	~~Tropospheric delay~~
~~I_i^k~~	~~Ionospheric delay~~
N_i^k	Phase ambiguity
Δ_{rel}	Relativistic corrections
b^k	Delays in satellite (cables, electronics)
b_i	Delays in receiver and antenna
m_i^k	Multipath, scattering, bending effects
ϵ_i^k	Measurement error

Satellite positions and clocks are known from ACs or IGS

Not existent for LEOs

Cancels out (first order only) when forming the ionosphere-free linear combination:

$$L_c = \frac{f_1^2}{f_1^2 - f_2^2} L_1 - \frac{f_2^2}{f_1^2 - f_2^2} L_2$$

Geometric Distance

Geometric distance ρ_{leo}^{k} is given by:

$$\rho_{leo}^{k} = \left|\boldsymbol{r}_{leo}(t_{leo}) - \boldsymbol{r}^{k}(t_{leo} - \tau_{leo}^{k})\right|$$

$\boldsymbol{r}_{leo}$ Inertial position of LEO antenna phase center at reception time

$\boldsymbol{r}^{k}$ Inertial position of GPS antenna phase center of satellite k at emission time

τ_{leo}^{k} Signal traveling time between the two phase center positions

Different ways to represent $\boldsymbol{r}_{leo}$:

- **Kinematic** orbit representation
- **Dynamic** or **reduced-dynamic** orbit representation

Kinematic Orbit Representation (1)

Satellite position $\boldsymbol{r}_{leo}(t_{leo})$ (in inertial frame) is given by:

$$\boldsymbol{r}_{leo}(t_{leo}) = \boldsymbol{R}(t_{leo}) \cdot (\boldsymbol{r}_{leo,e,0}(t_{leo}) + \delta\boldsymbol{r}_{leo,e,ant}(t_{leo}))$$

$\boldsymbol{R}$	Transformation matrix from Earth-fixed to inertial frame
$\boldsymbol{r}_{leo,e,0}$	LEO center of mass position in Earth-fixed frame
$\delta\boldsymbol{r}_{leo,e,ant}$	LEO antenna phase center offset in Earth-fixed frame

Kinematic positions $\boldsymbol{r}_{leo,e,0}$ are estimated for each **measurement epoch**:

- Measurement epochs **need not** to be identical with nominal epochs
- Positions are **independent** of models describing the LEO dynamics. Velocities cannot be provided

Kinematic Orbit Representation (2)

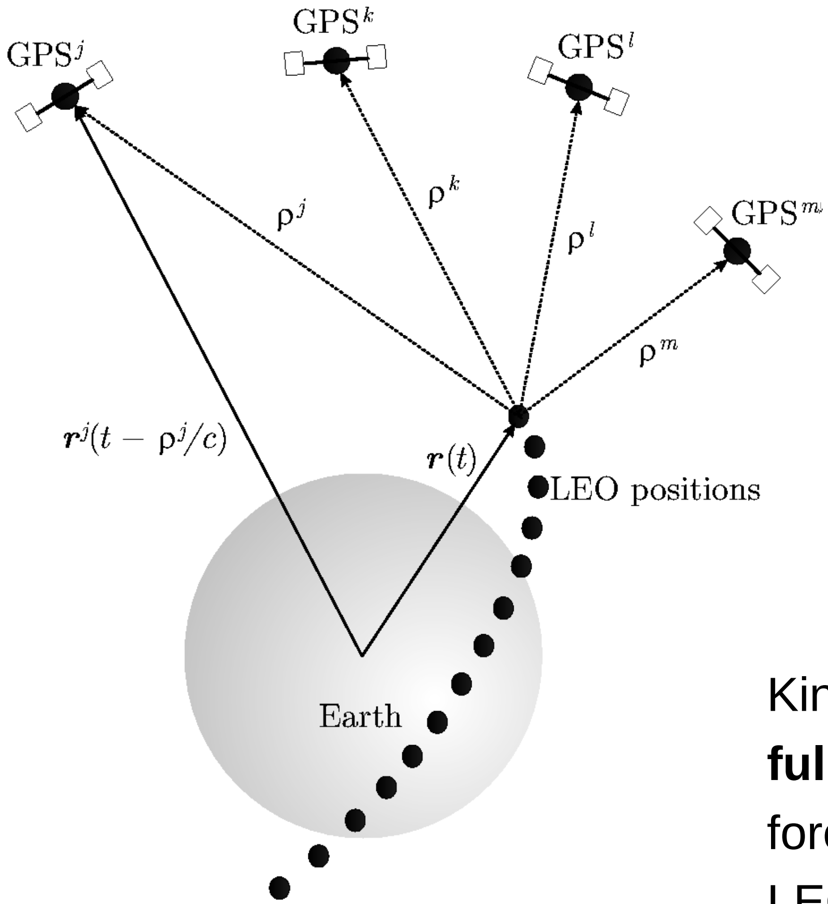

A kinematic orbit is an ephemeris at **discrete** measurement epochs

Kinematic positions are **fully independent** on the force models used for LEO orbit determination

(Švehla and Rothacher, 2004)

Kinematic Orbit Representation (3)

Measurement epochs
(in GPS time)

Positions (km)
(Earth-fixed)

Clock correction to
nominal epoch (μs),
e.g., to epoch
00:00:20

*	2016	6	1	0	0	17.99999974		
PL49	-2023.517746	-3061.130332	5742.844473	0.262691				
*	2016	6	1	0	0	18.99999989		
PL49	-2026.734429	-3066.703833	5738.746569	0.111976				
*	2016	6	1	0	0	19.99999974		
PL49	-2029.949393	-3072.273033	5734.641440	0.261262				
*	2016	6	1	0	0	20.99999979		
PL49	-2033.162630	-3077.837924	5730.529099	0.210548				
*	2016	6	1	0	0	21.99999984		
PL49	-2036.374136	-3083.398504	5726.409546	0.159835				
*	2016	6	1	0	0	22.99999979		
PL49	-2039.583909	-3088.954755	5722.282787	0.209119				
*	2016	6	1	0	0	23.99999984		
PL49	-2042.791949	-3094.506686	5718.148843	0.158440				
*	2016	6	1	0	0	24.99999979		
PL49	-2045.998248	-3100.054291	5714.007709	0.207778				
*	2016	6	1	0	0	25.99999974		
PL49	-2049.202791	-3105.597545	5709.859370	0.257064				
*	2016	6	1	0	0	26.99999979		
PL49	-2052.405584	-3111.136450	5705.703844	0.206352				

Excerpt of kinematic Swarm-C positions at begin of 1 June, 2016

The kinematic orbits may be downloaded at ftp://ftp.unibe.ch/aiub/LEO_ORBITS/

Dynamic Orbit Representation (1)

Satellite position $\boldsymbol{r}_{leo}(t_{leo})$ (in inertial frame) is given by:

$$\boldsymbol{r}_{leo}(t_{leo}) = \boldsymbol{r}_{leo,0}(t_{leo}; a, e, i, \Omega, \omega, u_0; Q_1, ..., Q_d) + \delta\boldsymbol{r}_{leo,ant}(t_{leo})$$

$\boldsymbol{r}_{leo,0}$	LEO center of mass position
$\delta\boldsymbol{r}_{leo,ant}$	LEO antenna phase center offset
$a, e, i, \Omega, \omega, u_0$	LEO initial osculating orbital elements
$Q_1, ..., Q_d$	LEO dynamical parameters

Satellite trajectory $\boldsymbol{r}_{leo,0}$ is a particular solution of an **equation of motion**

- One set of **initial conditions** (orbital elements) is estimated per arc. Dynamical parameters of the force model on request

Dynamic Orbit Representation (2)

Equation of motion (in inertial frame) is given by:

$$\ddot{\boldsymbol{r}} = -GM\frac{\boldsymbol{r}}{r^3} + \boldsymbol{f}_1(t, \boldsymbol{r}, \dot{\boldsymbol{r}}, Q_1, ..., Q_d)$$

with initial conditions

$$\boldsymbol{r}(t_0) = \boldsymbol{r}(a, e, i, \Omega, \omega, u_0; t_0)$$
$$\dot{\boldsymbol{r}}(t_0) = \dot{\boldsymbol{r}}(a, e, i, \Omega, \omega, u_0; t_0)$$

The **acceleration** $\boldsymbol{f}_1$ consists of **gravitational** and **non-gravitational** perturbations taken into account to model the satellite trajectory. Unknown parameters $Q_1, ..., Q_d$ of force models may appear in the equation of motion together with deterministic (known) accelerations given by analytical models.

Osculating Orbital Elements

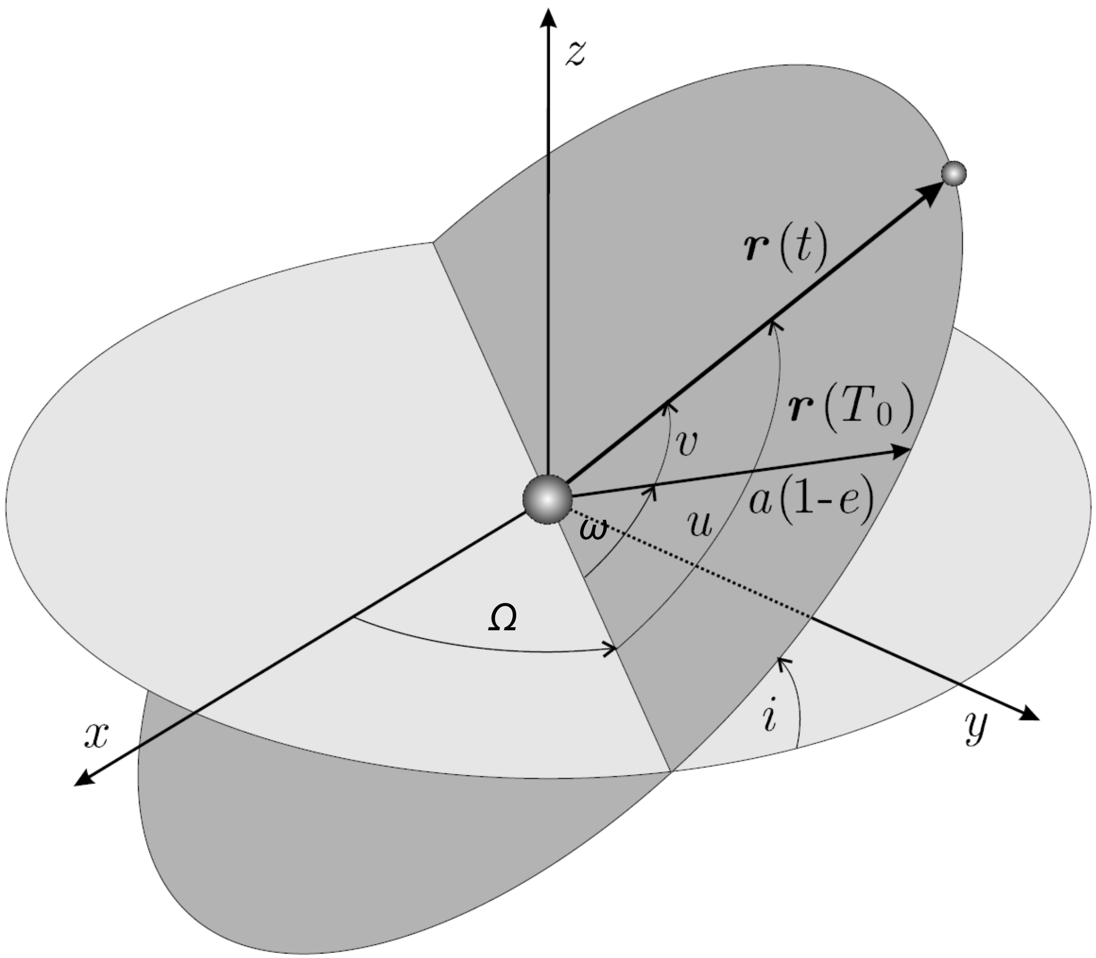

(Beutler, 2005)

Perturbing Accelerations of a LEO Satellite

Force	**Acceleration** (m/s²)
Central term of Earth‘s gravity field	8.42
Oblateness of Earth‘s gravity field	0.015
Atmospheric drag	0.00000079
Higher order terms of Earth‘s gravity field	0.00025
Attraction from the Moon	0.0000054
Attraction from the Sun	0.0000005
Direct solar radiation pressure	0.000000097
...	...

Dynamic Orbit Representation (3)

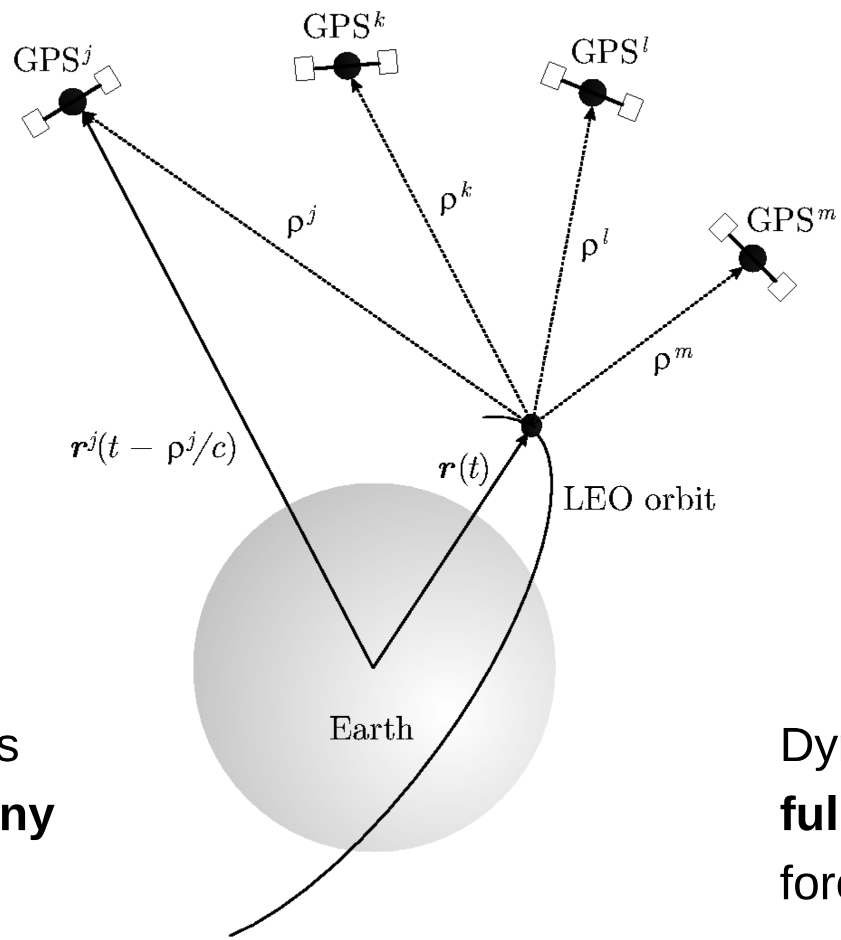

Dynamic orbit positions may be computed at **any epoch** within the arc

Dynamic positions are **fully dependent** on the force models used, e.g., on the gravity field model

Reduced-Dynamic Orbit Representation (1)

Equation of motion (in inertial frame) is given by:

$$\ddot{\boldsymbol{r}} = -GM\frac{\boldsymbol{r}}{r^3} + \boldsymbol{f}_1(t, \boldsymbol{r}, \dot{\boldsymbol{r}}, Q_1, ..., Q_d, P_1, ..., P_s)$$

$P_1, ..., P_s$ Pseudo-stochastic parameters

Pseudo-stochastic parameters are:

- additional empirical parameters characterized by a priori known **statistical properties**, e.g., by expectation values and a priori variances

- useful to **compensate** for deficiencies in dynamic models, e.g., deficiencies in models describing non-gravitational accelerations

- often set up as **piecewise constant accelerations** to ensure that satellite trajectories are continuous and differentiable at any epoch

Reduced-Dynamic Orbit Representation (2)

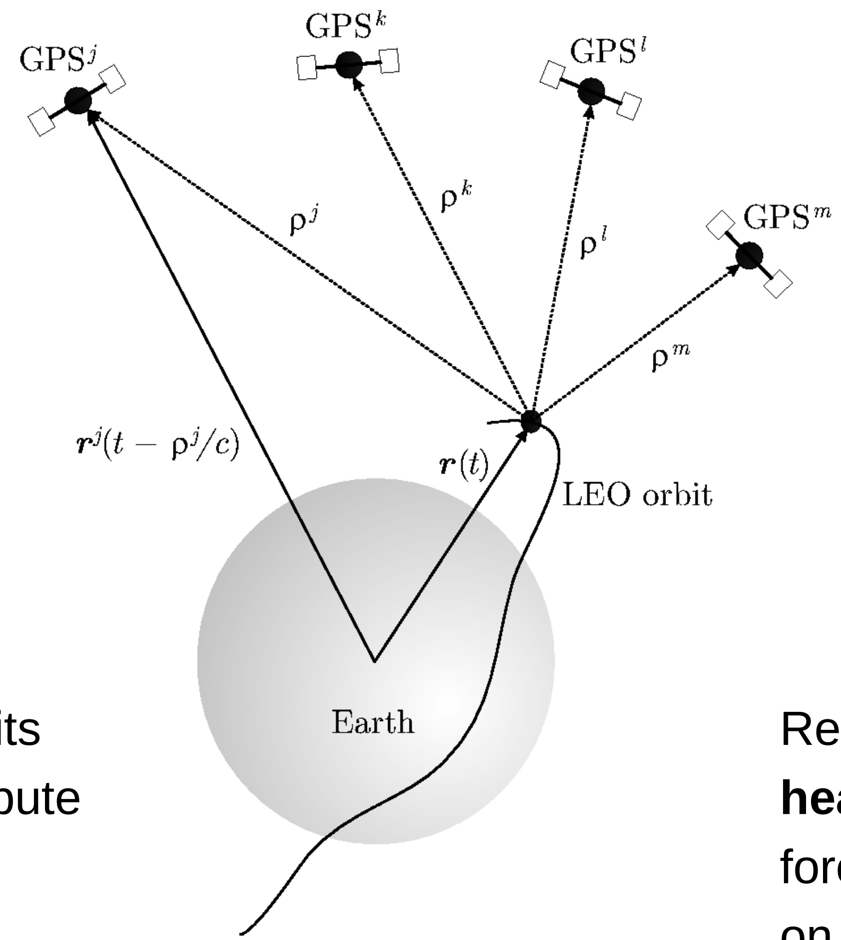

Reduced-dynamic orbits are well suited to compute LEO orbits of **highest quality**

(Jäggi et al., 2006; Jäggi, 2007)

Reduced-dynamic orbits **heavily depend** on the force models used, e.g., on the gravity field model

Reduced-dynamic Orbit Representation (3)

Position epochs
(in GPS time)

Positions (km) &
Velocities (dm/s)
(Earth-fixed)

```
*  2016  6  1  0  0  0.00000000
PL49  -1965.328762  -2960.079621   5815.366063 999999.999999
VL49 -32476.530949 -56518.428574 -39633.949261 999999.999999
*  2016  6  1  0  0 10.00000000
PL49  -1997.722965  -3016.388318   5775.367094 999999.999999
VL49 -32311.097194 -56097.834133 -40363.154274 999999.999999
*  2016  6  1  0  0 20.00000000
PL49  -2029.949403  -3072.273033   5734.641439 999999.999999
VL49 -32141.000143 -55670.464832 -41087.301898 999999.999999
*  2016  6  1  0  0 30.00000000
PL49  -2062.003415  -3127.727011   5693.194205 999999.999999
VL49 -31966.250891 -55236.380456 -41806.300697 999999.999999
*  2016  6  1  0  0 40.00000000
PL49  -2093.880357  -3182.743574   5651.030585 999999.999999
VL49 -31786.861194 -54795.641569 -42520.059993 999999.999999
*  2016  6  1  0  0 50.00000000
PL49  -2125.575594  -3237.316095   5608.155863 999999.999999
VL49 -31602.843520 -54348.309592 -43228.489711 999999.999999
*  2016  6  1  0  1  0.00000000
PL49  -2157.084506  -3291.438018   5564.575411 999999.999999
VL49 -31414.211010 -53894.446726 -43931.500489 999999.999999
```

Clock corrections
are not provided

Excerpt of reduced-dynamic Swarm-C positions at begin of 1 June, 2016

LEO Sensor Offsets

Phase center offsets $\delta \boldsymbol{r}_{leo,ant}$:

- are needed in the inertial or Earth-fixed frame and have to be transformed from the satellite frame using **attitude data** from the star-trackers

- consist of a frequency-independent **instrument offset**, e.g., defined by the center of the instrument‘s mounting plane (CMP) in the satellite frame

- consist of frequency-dependent **phase center offsets** (PCOs), e.g., defined wrt the center of the instrument‘s mounting plane in the antenna frame (ARF)

- consist of frequency-dependent **phase center variations** (PCVs) varying with the direction of the incoming signal, e.g., defined wrt the PCOs in the antenna frame

LEO Sensor Offsets

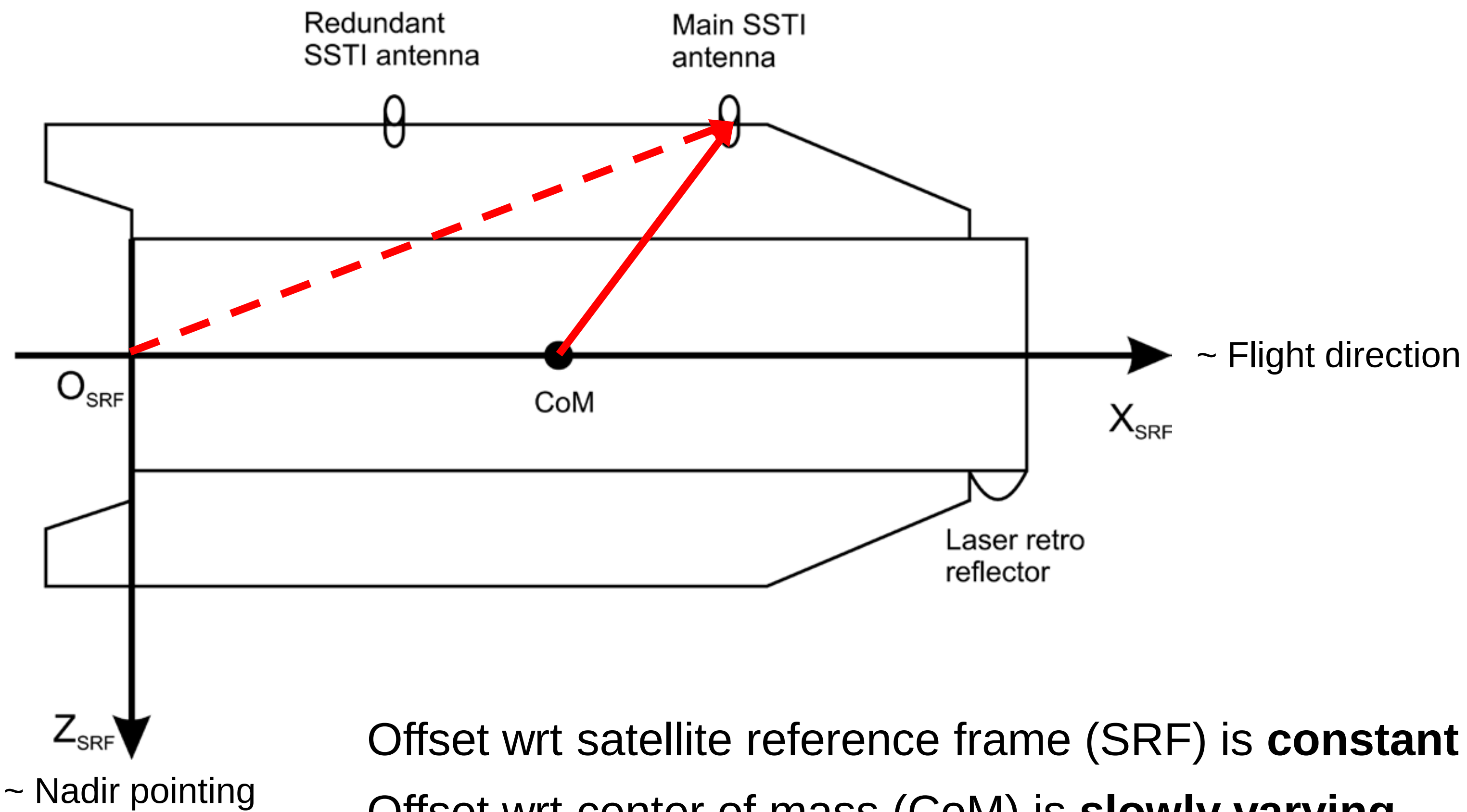

Offset wrt satellite reference frame (SRF) is **constant**

Offset wrt center of mass (CoM) is **slowly varying**

Spaceborne GPS Antennas: GOCE

L1, L2, Lc phase center offsets

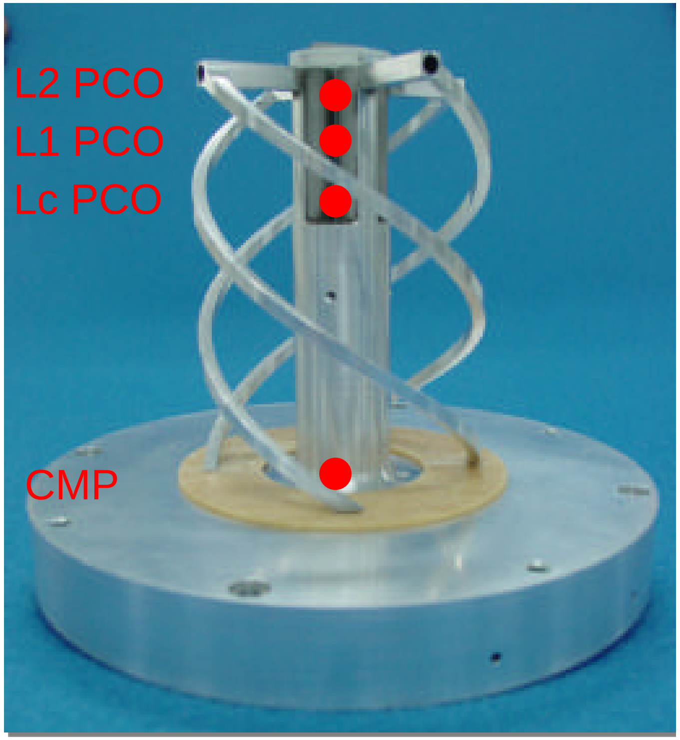

Measured from ground calibration in anechoic chamber

Lc phase center variations

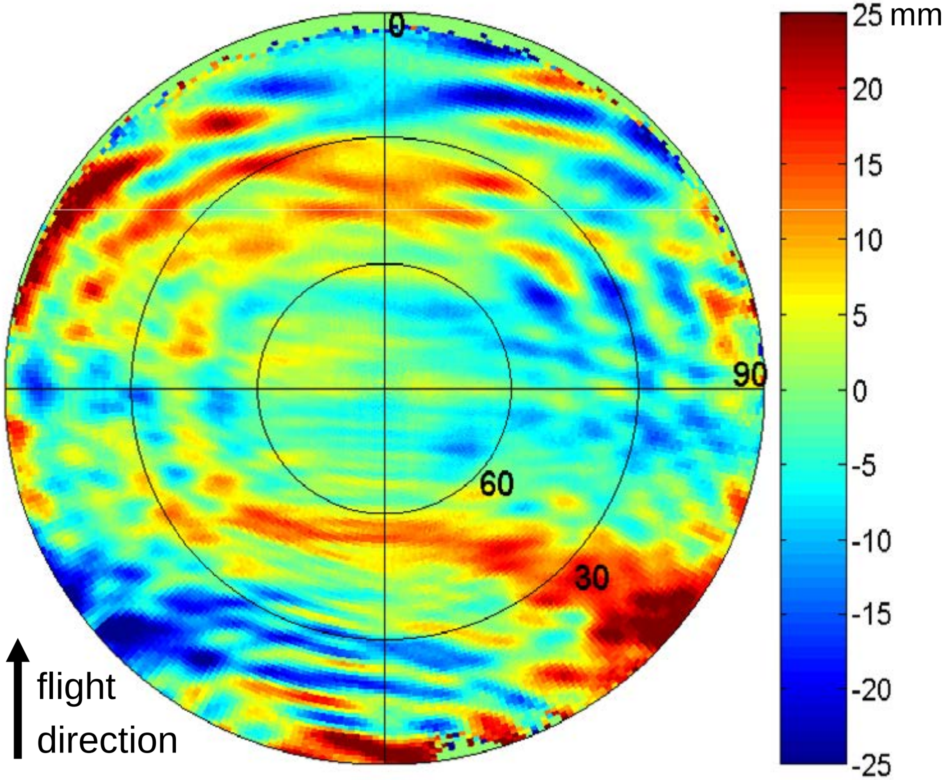

Empirically derived during orbit determination according to Jäggi et al. (2009)

Spaceborne GPS Antennas: Swarm

Swarm GPS antenna

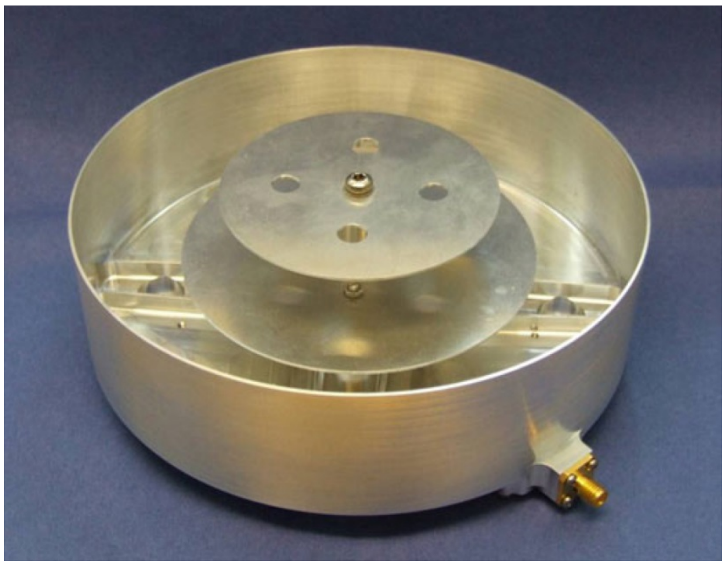

Multipath shall be minimzed by chokering

L_{if} phase center variations

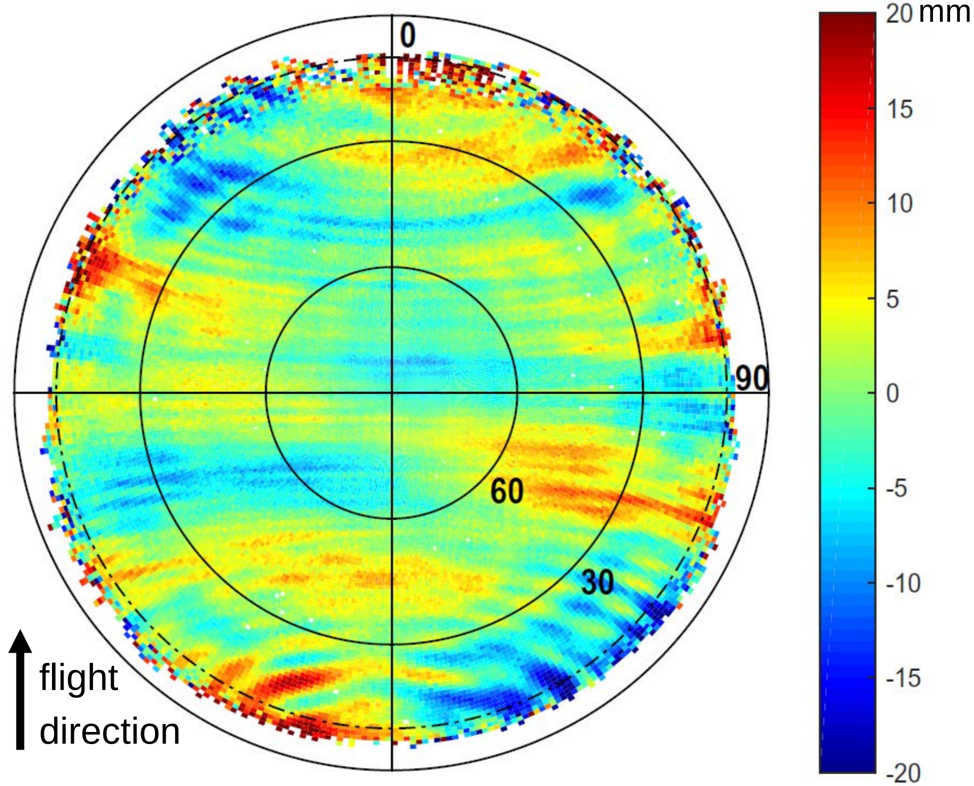

Empirically derived during orbit determination according to Jäggi et al. (2009)

Visualization of Orbit Solutions

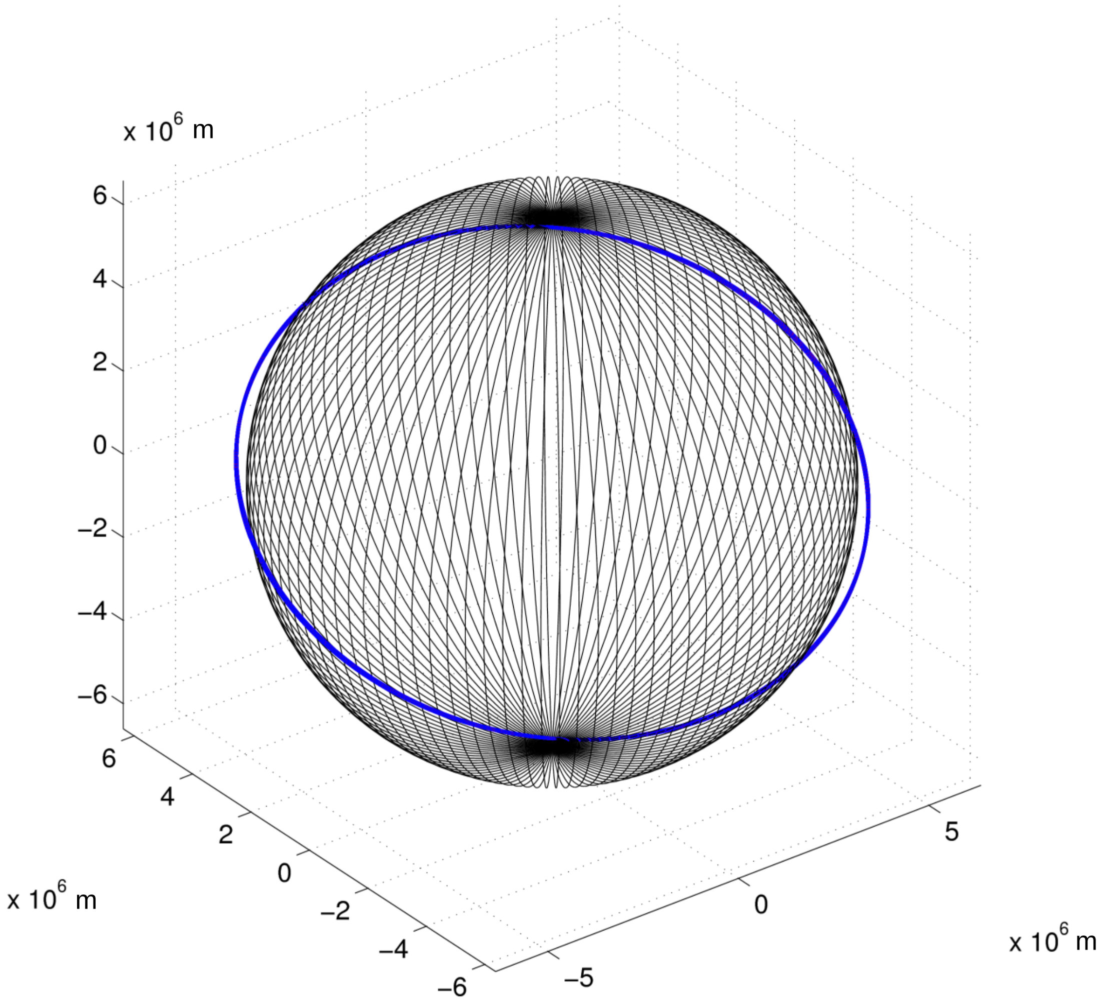

It is more instructive to look at differences between orbits in well suited coordinate systems …

Co-Rotating Orbital Frames

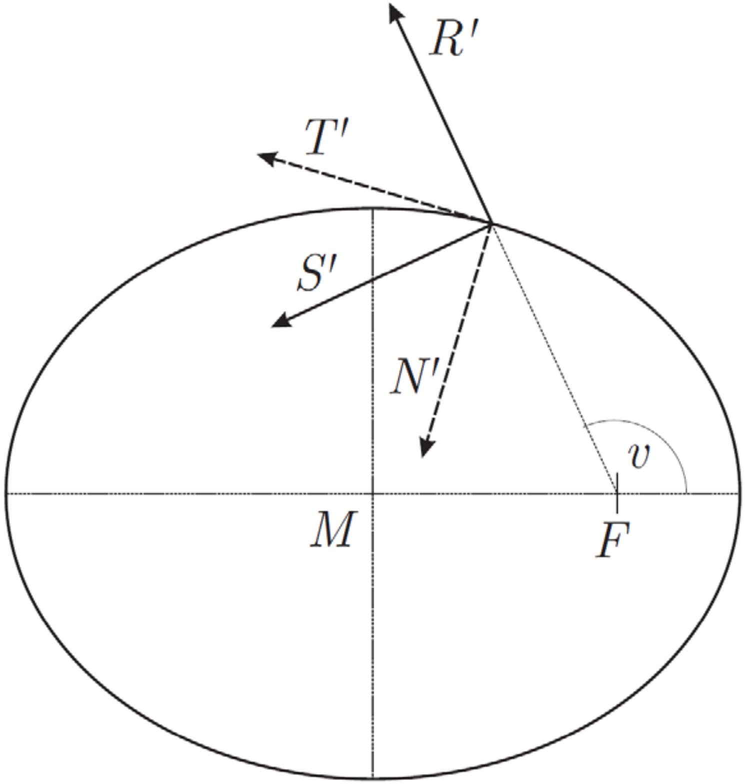

R, S, C unit vectors are pointing:

- into the radial direction
- normal to **R** in the orbital plane
- normal to the orbital plane (cross-track)

T, N, C unit vectors are pointing:

- into the tangential (along-track) direction
- normal to **T** in the orbital plane
- normal to the orbital plane (cross-track)

Small eccentricities: **S**~**T** (velocity direction)

(Beutler, 2005)

Orbit Differences KIN-RD (Swarm-C)

Differences at epochs of kin. positions

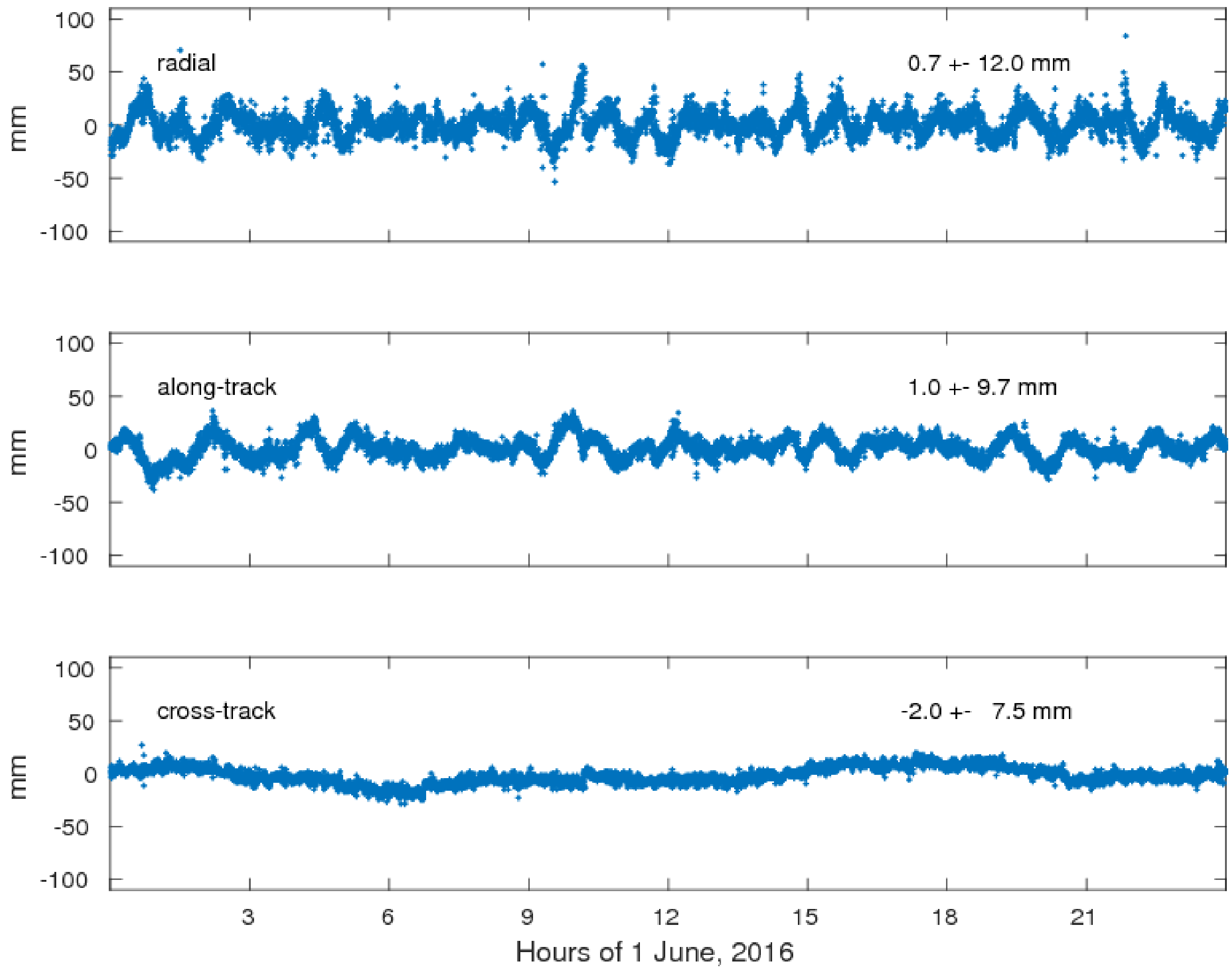

Pseudo-Stochastic Accelerations (GOCE)

Largest signal
due to air-drag

First drag-free
flight on 7-May

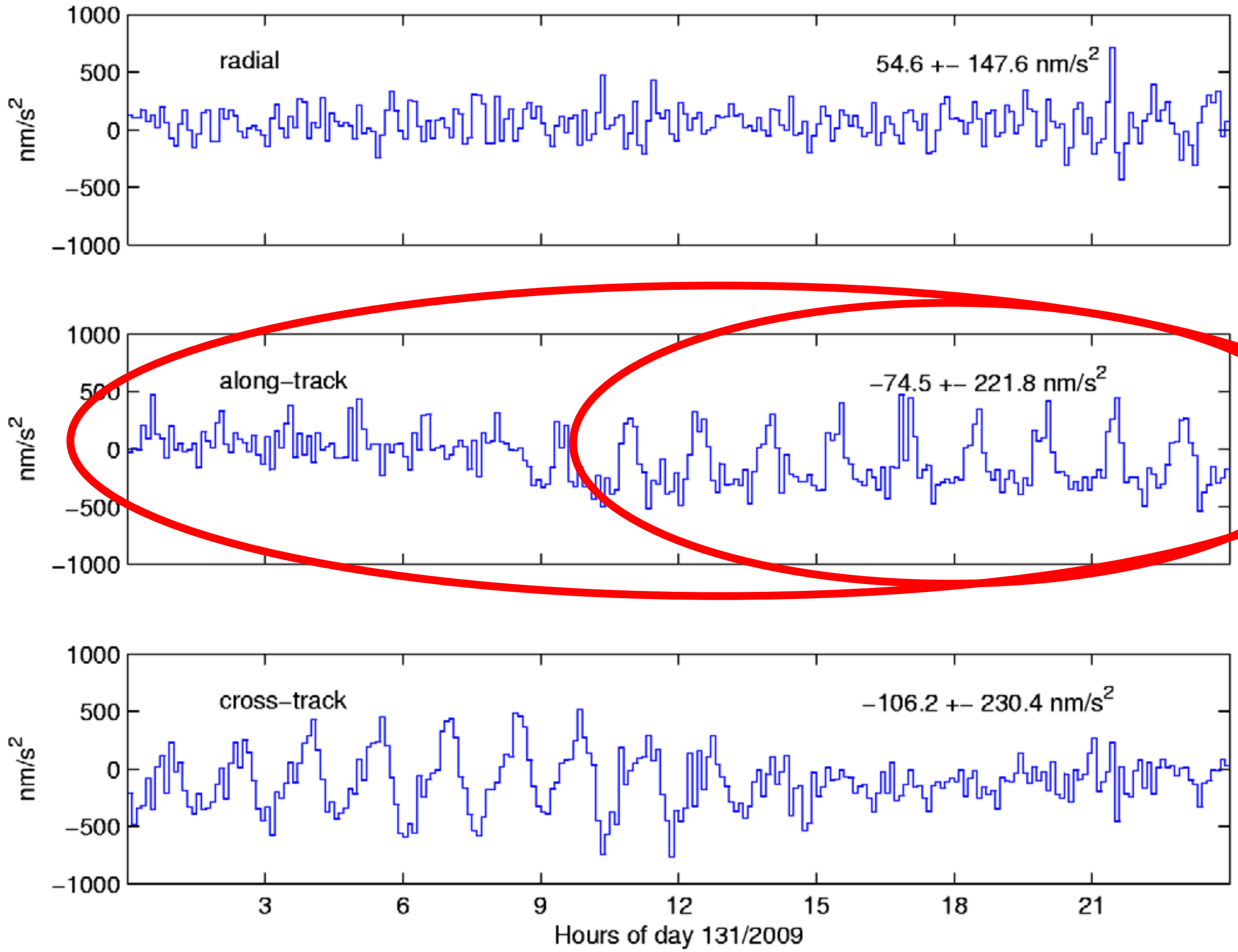

Kinematic Orbit Validation with SLR

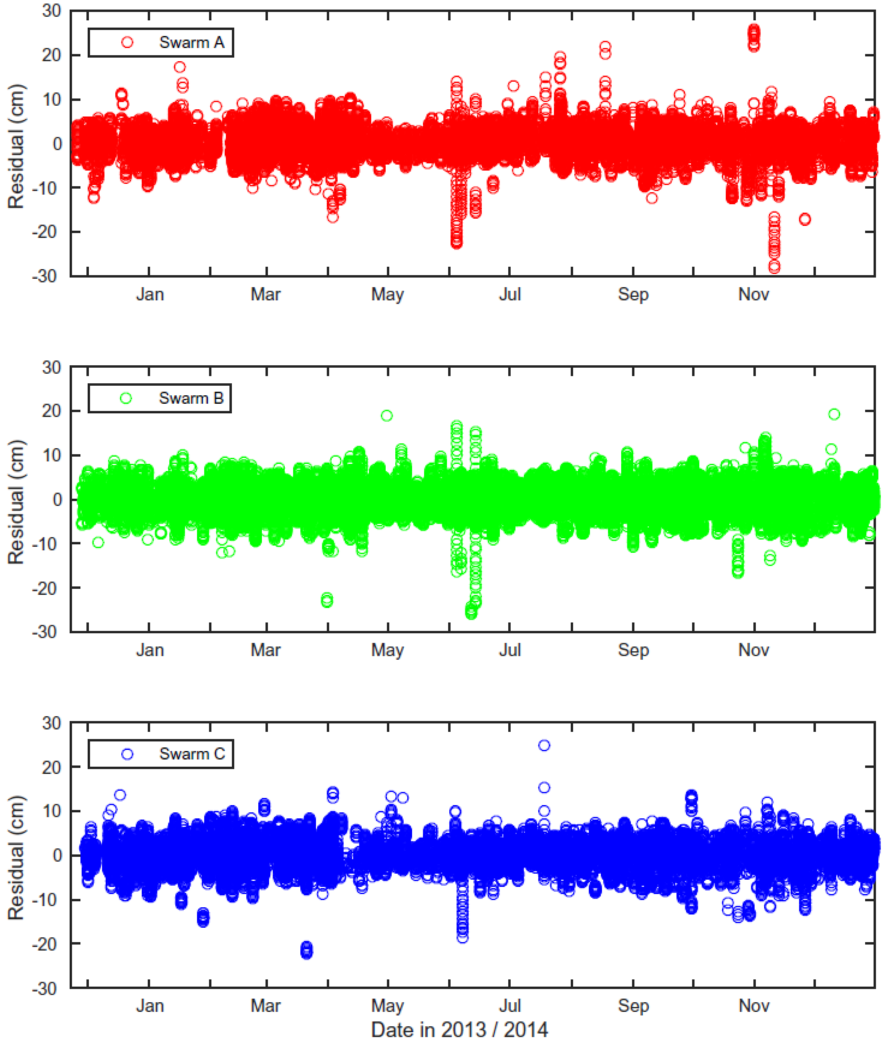

SLR statistics:

Mean ± RMS (cm)

0.27 ± 3.25 cm

0.10 ± 2.74 cm

0.06 ± 3.11 cm

(Jäggi et al., 2016)

Consequences of Ionospheric Effects in Orbits

For GOCE systematic effects around the geomagnetic equator were observed in the ionosphere-free GPS phase residuals **=> affects kinematic positions**

Degradation of kinematic positions around the geomagnetic equator propagates into gravity field solutions.

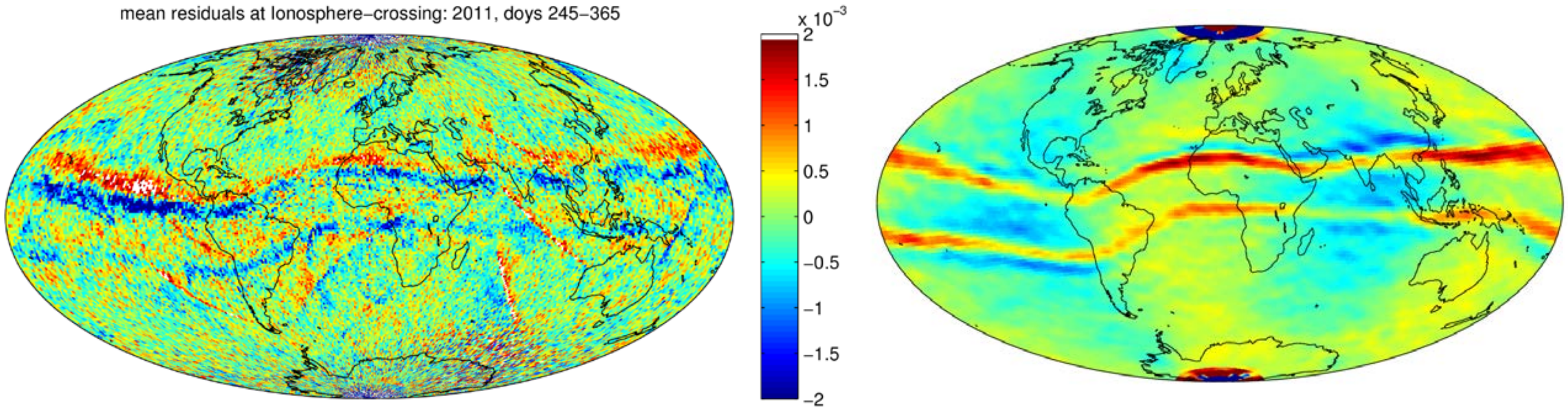

Phase observation residuals (- 2 mm … +2 mm) mapped to the ionosphere piercing point

Geoid height differences (−5 cm … 5 cm); **R4 period**

(Jäggi et al., 2015)

Situation for Swarm

Original GPS Data
(13 months)

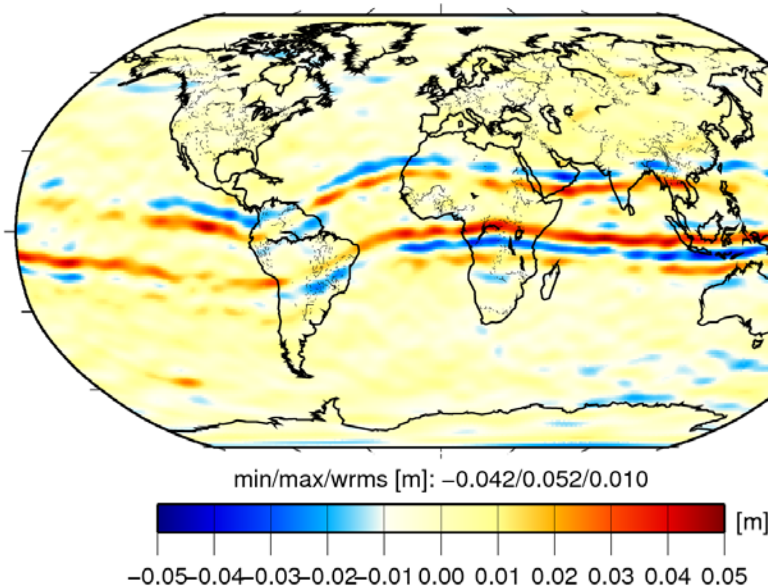

Screened GPS Data
(18 months)

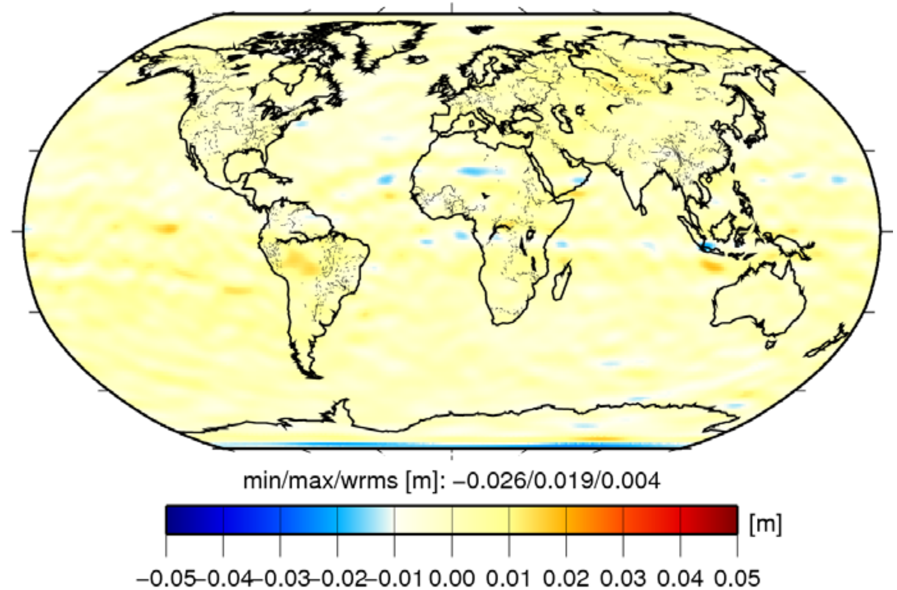

(Differences wrt GOCO05S, 400 km Gauss smoothing adopted)

Systematic signatures along the geomagnetic equator may be efficiently reduced for static Swarm gravity field recovery when screening the raw RINEX GPS data files with the ΔL_{gf} criterion.

(Jäggi et al., 2016)

Situation for other LEO Satellites

Original GPS Data
(Swarm)

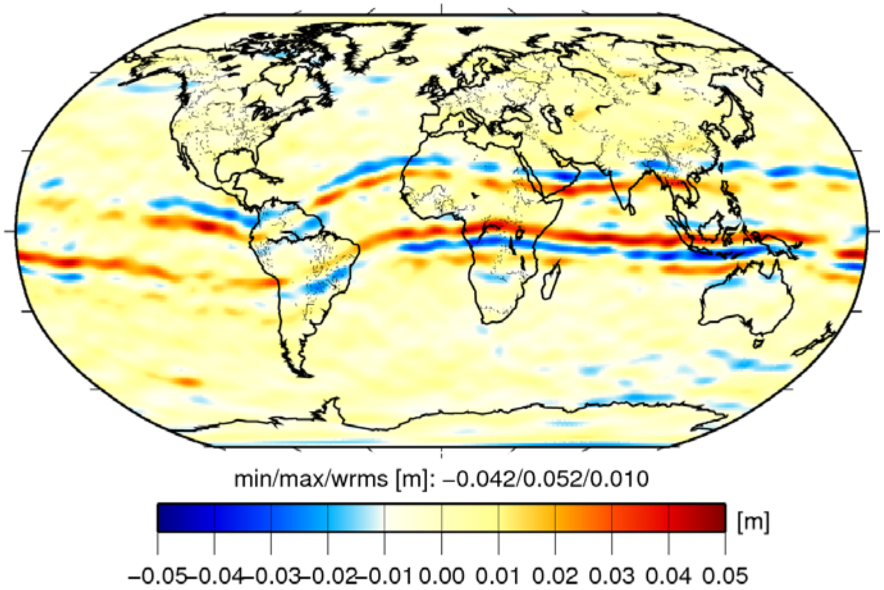

Original GPS Data
(GRACE)

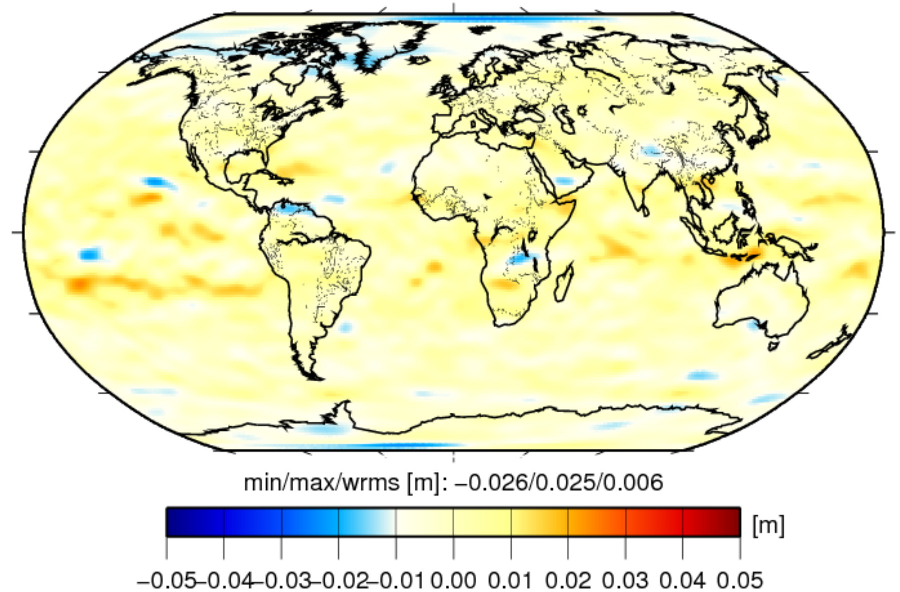

(Differences wrt GOCO05S, 400 km Gauss smoothing adopted)

Systematic signatures along the geomagnetic equator are not visible when using original L1B RINEX GPS data files from the GRACE mission.

(Jäggi et al., 2016)

Data Gaps in RINEX Files

GRACE-B, doy 060-090, 2014

Swarm-A, doy 060-090, 2014

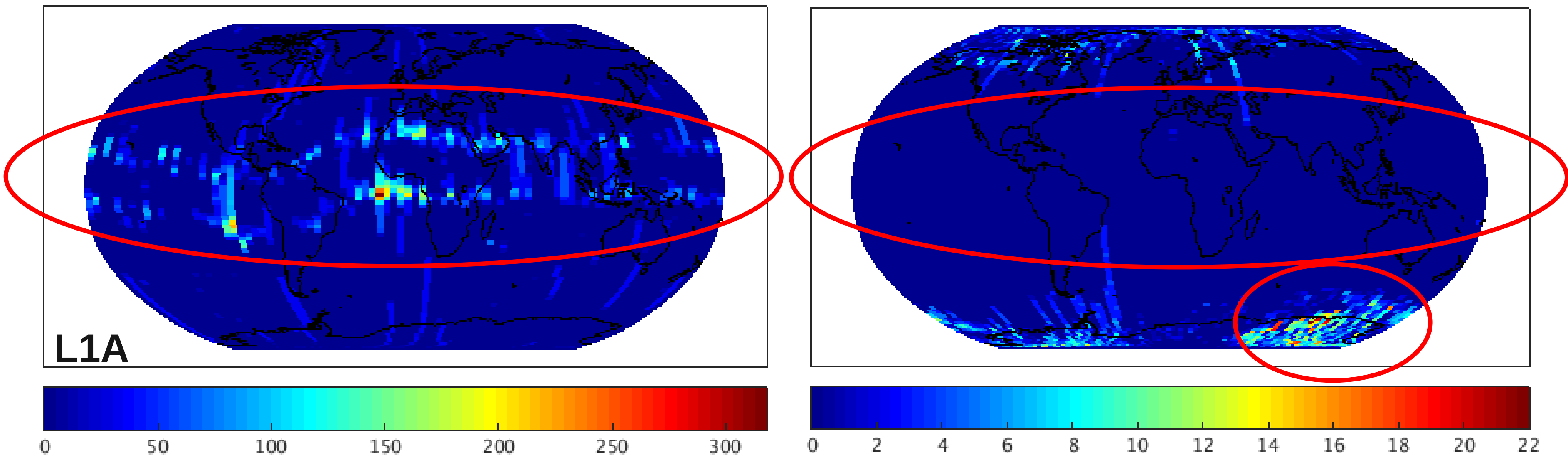

Significant amounts of data are missing in GRACE L1B RINEX files

=> problematic signatures cannot propagate into gravity field.

Swarm RINEX files are more complete (gaps only over the poles)

=> problematic signatures do propagate into the gravity field.

(Jäggi et al., 2016)

Ionospheric Signatures in GPS Linear Combinations

South-pole pass

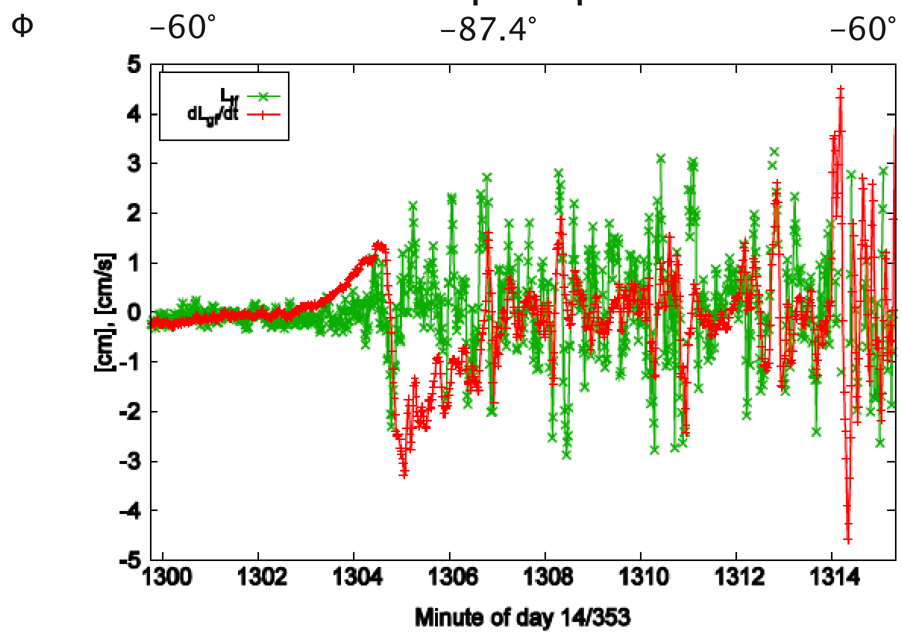

Equatorial pass

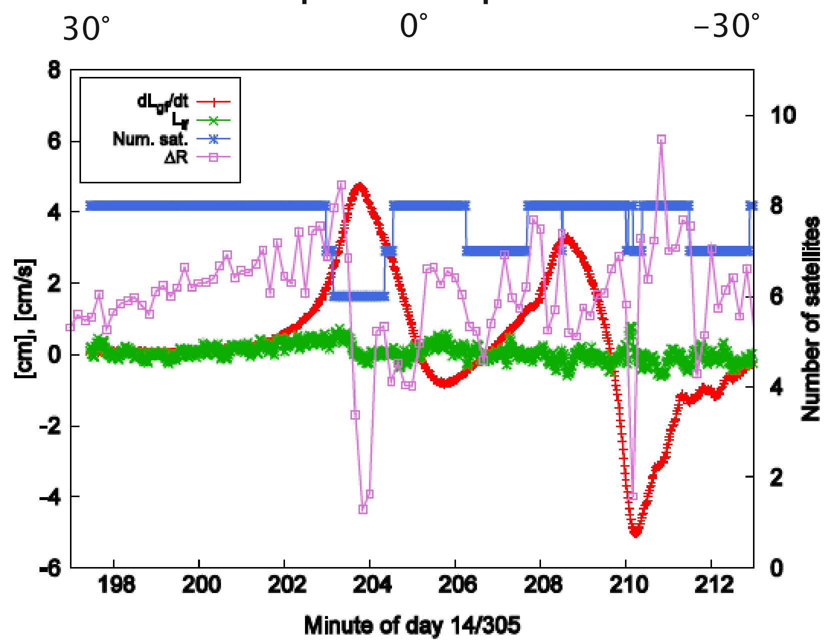

L_{if} :
Phase residuals of ionosphere-free linear combination L_{if} from kinematic POD

ΔL_{gf}:
Epoch-to-epoch difference of geometry-free linear combination

Number of satellites used for kinematic positioning

Radial difference between kinematic and reduced-dynamic orbit

(Arnold et al., 2016)

Global Ionosphere behavior

RMS of ΔL_{gf} (full signal)

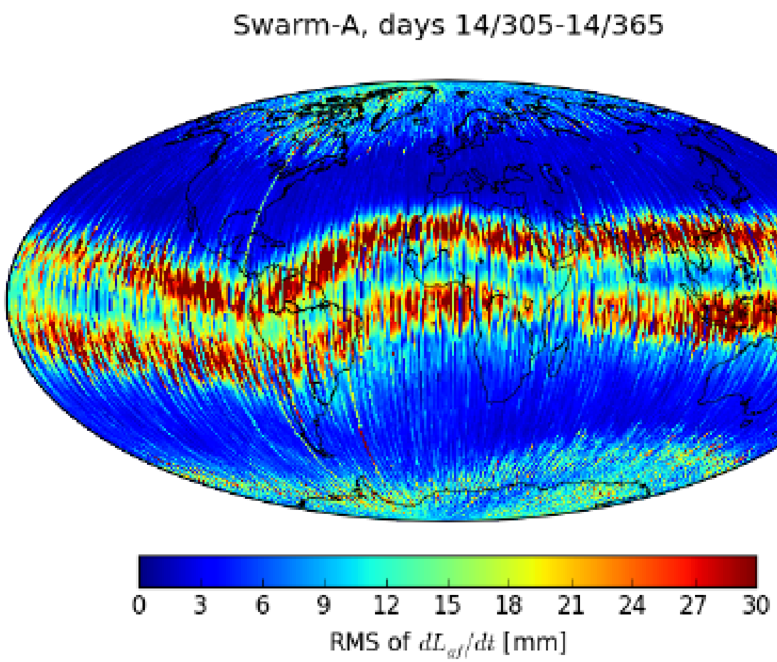

RMS of ΔL_{gf} (high-pass)

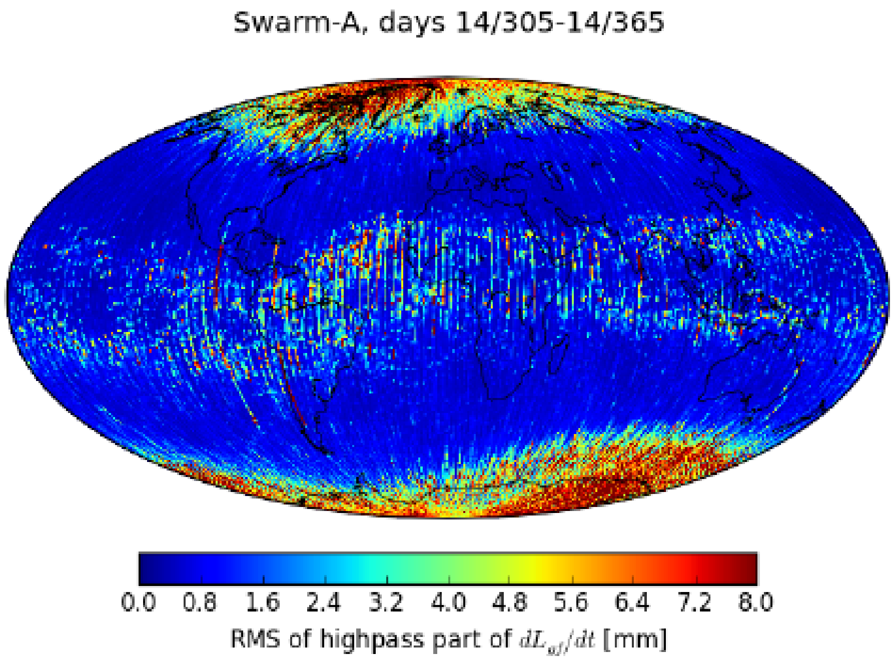

Equatorial regions are mainly governed by "deterministic" features
=> Systematic gravity field errors

Polar regions are mainly governed by "scintillation-like" features
=> Gravity field is hardly affected

(Arnold et al., 2016)

Upgrades in the Swarm GPS Receiver Settings

A wider L2 carrier loop bandwidth increases the robustness of the L2 carrier phase tracking. In an attempt to improve the performance of the Swarm GPS receivers, the L2 carrier loop bandwidth was e.g. increased several times:

	Swarm A	Swarm B	Swarm C
Before 6 May 2015	0.25Hz	0.25Hz	0.25Hz
6 May 2015			0.25Hz → 0.5Hz
8 October 2015	0.25Hz → 0.5Hz		
10 October 2015		0.25Hz → 0.5Hz	
23 June 2016			0.5Hz → 0.75Hz
11 August 2016	0.5Hz → 0.75Hz		0.75Hz → 1.0Hz

One of the three settings (0.5 Hz, 0.75 Hz, 1.0 Hz) is expected to be optimal and shall eventually be implemented on all Swarm satellites.

Impact on Gravity Field Solutions (June 2015)

Screened GPS data (ΔL_{gf} > 2cm/s excl.)

Original GPS data

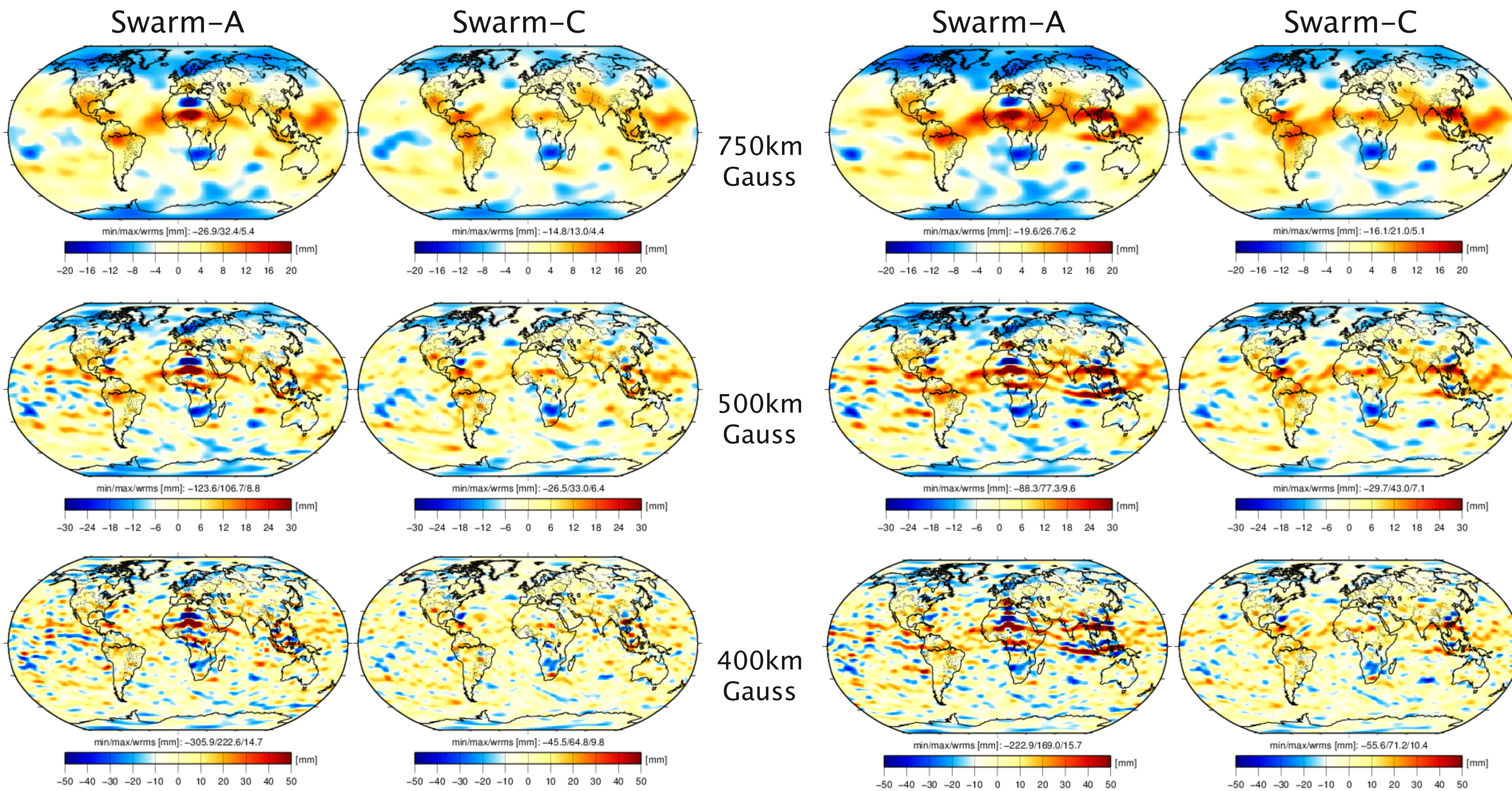

(Dahle et al., 2016)

Impact on Missing observations (June 2015)

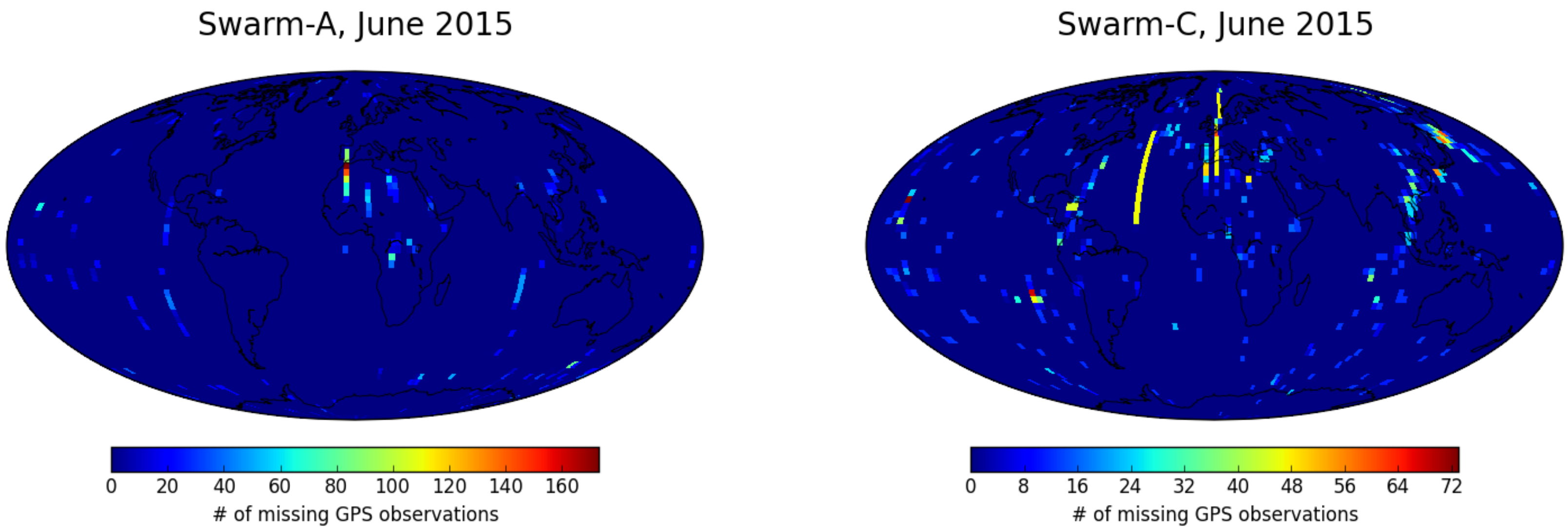

- No obvious gaps for Swarm-C along geomagnetic equator.
- Reduction of artefacts in gravity field solutions is therefore not due to data gaps along geomagnetic equator.
- This indicates that the equatorial GPS data were indeed “corrupted” before the tracking loop changes. With improved settings of the tracking loop the problem seems to be largely mitigated**.**

(Dahle et al., 2016)

Comparison to RINEX Screening

Original GPS data

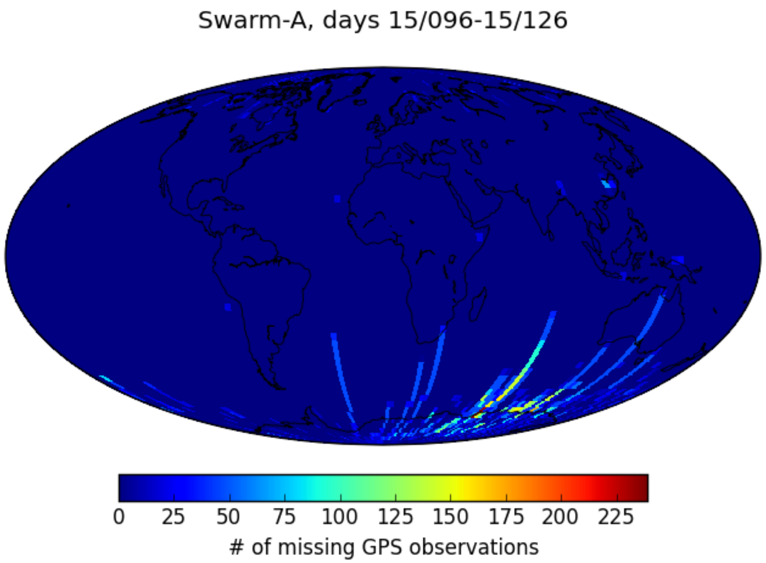

Screened GPS data

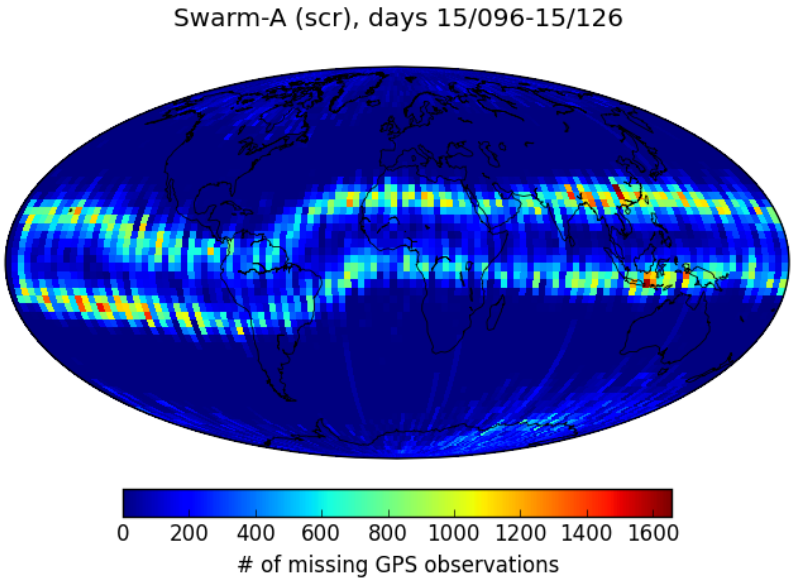

- RINEX screening is useful for gravity field recovery, but rejects a lot (too much) of GPS data, at least in the way as implemented so far.
- Improved tracking loop settings are most promising to use the full amount of GPS data while significantly reducing the observed artefacts in the gravity field recovery.

(Dahle et al., 2016)

Outlook: Time-Variable Gravity from Swarm

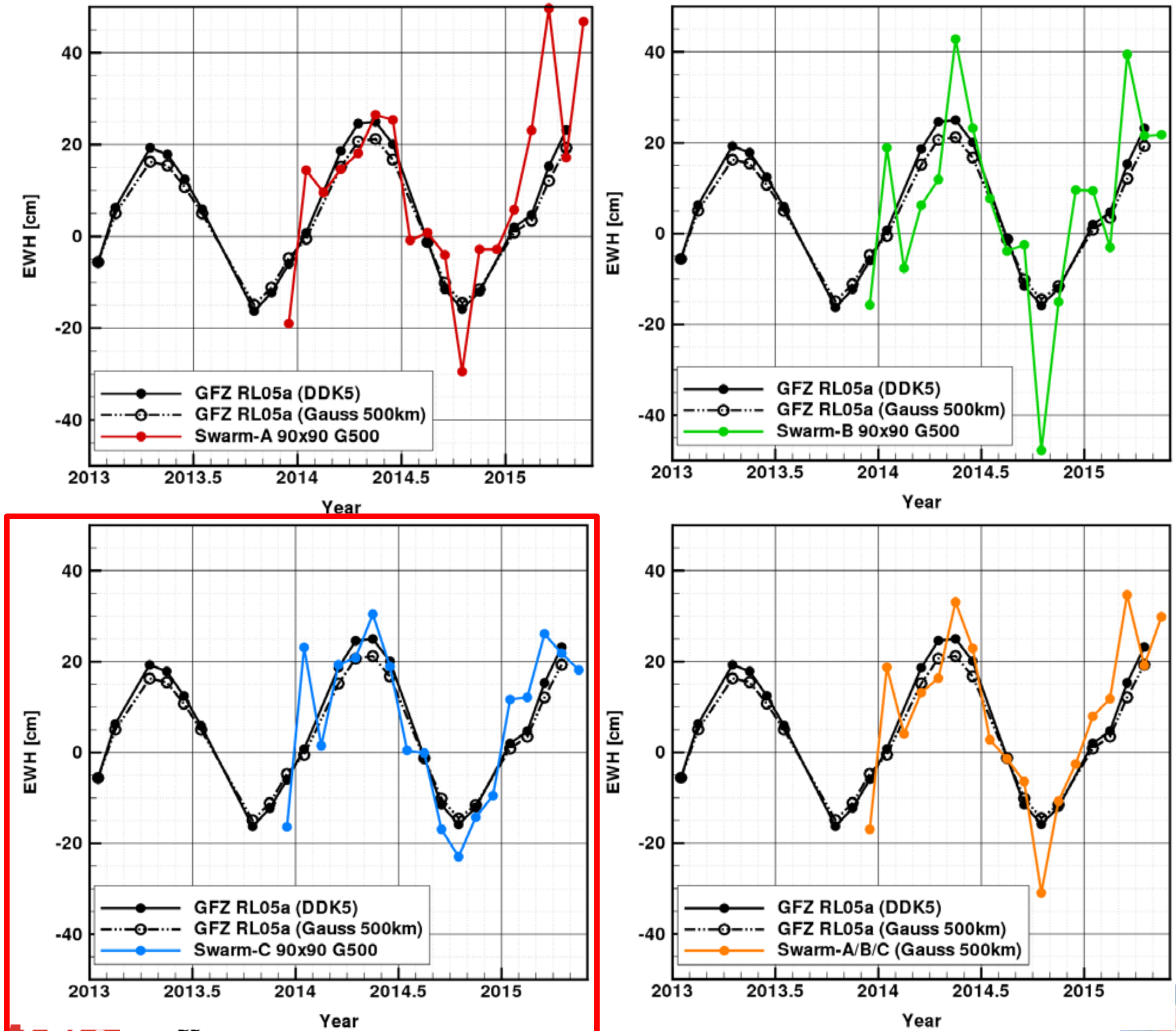

"True" signal:

- GFZ-RL05a (DDK5-filtered)

"Comparison" signal:

- GFZ-RL05a (500km Gauss)

Swarm signal:

- 90x90 solutions (Gauss-filtered)

Result:

- Best agreement for Swarm-C

(Jäggi et al., 2016)

Outlook: Time-Variable Gravity from Swarm

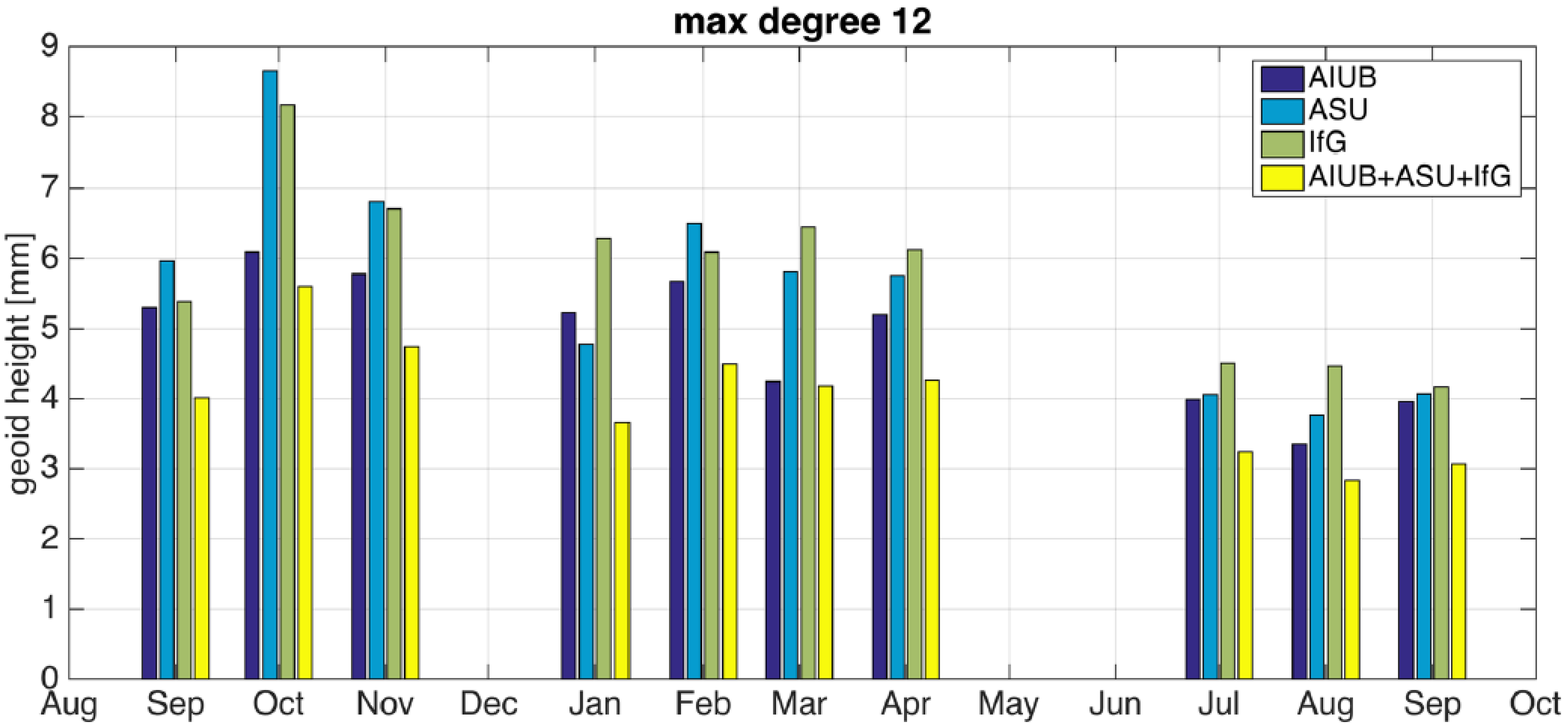

- Solutions based on AIUB orbits show a very good performance. This is probably mainly related to the quality of the underlying kinematic orbits.
- Combination of solutions from different groups (using different orbits and approaches for gravity field recovery) show a further reduced noise.

(Teixeira da Encarnação et al., 2016)

Outlook: Time-Variable Gravity from Non-Dedicated Satellites

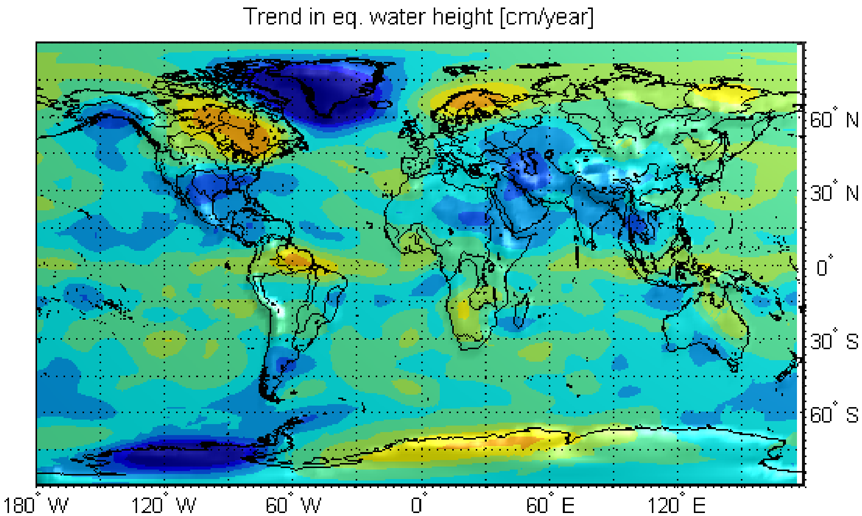

hl-SST

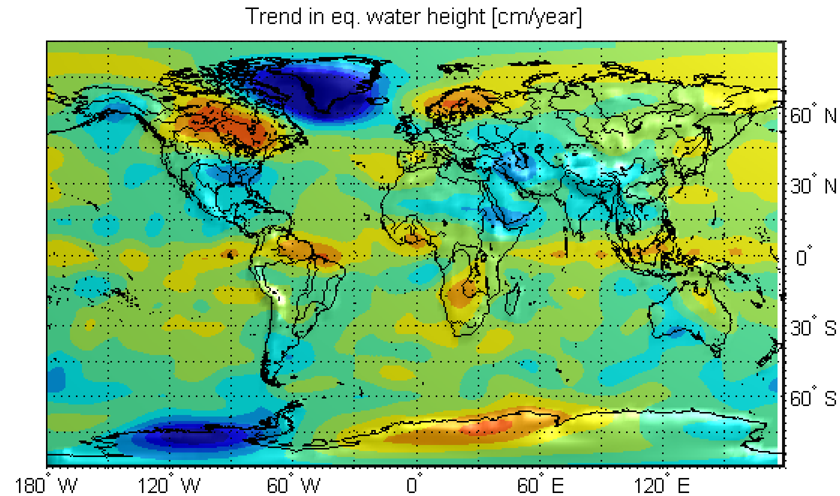

SLR+hl-SST

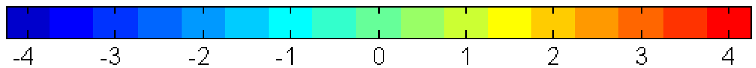

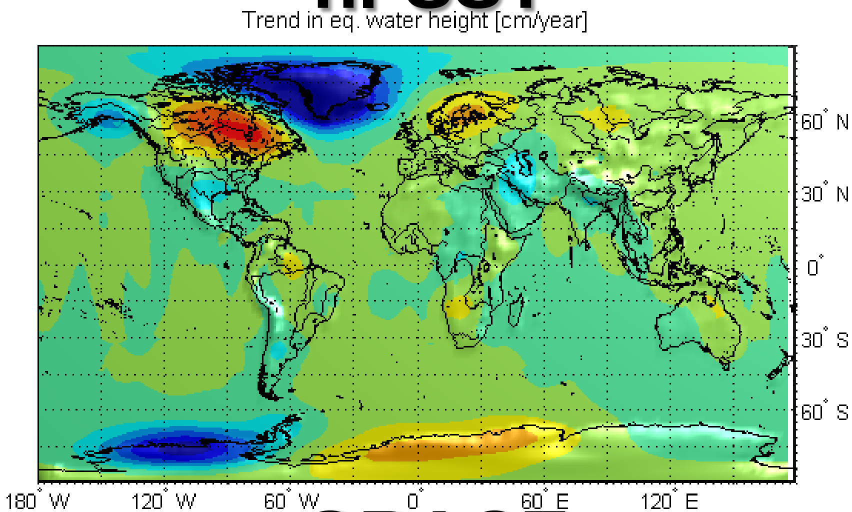

GRACE

Combination of hl-SST solutions with SLR reduces the variations over oceans and some spurious signals.

(Sośnica et al., 2014)


Thank you for your attention

Literature (1)

Arnold, D., C. Dahle, A. Jäggi, G. Beutler, U. Meyer; 2016: Impact of the ionosphere on GPS-based precise orbit determination of Low Earth Orbiters. ESA Living Planet Symposium, Prague, Czech Republic, May 09 -13, 2016, available at http://www.bernese.unibe.ch/publist/2016/post/Iono_LS16.pdf

Beutler, G. (2005) Methods of Celestial Mechanics. Vol 1: Physical, Mathematical, and Numerical Principles. Springer, ISBN 3-540-40749-9

Blewitt, G. (1997): Basics of the GPS Technique: Observation Equations, in *Geodetic Applications of GPS*, Swedish Land Survey, pp. 10-54, available at http://www.nbmg.unr.edu/staff/pdfs/blewitt basics of gps.pdf

Bock, H., R. Dach, A. Jäggi, G. Beutler (2009): High-rate GPS clock corrections from CODE: Support of 1 Hz applications. *Journal of Geodesy*, 83(11), 1083-1094, doi: 10.1007/s00190-009-0326-1

Dach, R., E. Brockmann, S. Schaer, G. Beutler, M. Meindl, L. Prange, H. Bock, A. Jäggi, L. Ostini (2009): GNSS processing at CODE: status report, *Journal of Geodesy*, 83(3-4), 353-366, doi: 10.1007/s00190-008-0281-2

Literature (2)

Dahle, C., D. Arnold, A. Jäggi (2016): Impact of tracking loop settings of the Swarm GPS receiver on orbit and gravity field results, *Advances in Space Research*, in preparation

Jäggi, A., U. Hugentobler, G. Beutler (2006): Pseudo-stochastic orbit modeling techniques for low-Earth satellites. *Journal of Geodesy*, 80(1), 47-60, doi: 10.1007/s00190-006-0029-9

Jäggi, A. (2007): Pseudo-Stochastic Orbit Modeling of Low Earth Satellites Using the Global Positioning System. *Geodätisch-geophysikalische Arbeiten in der Schweiz*, 73, Schweizerische Geodätische Kommission, available at http://www.sgc.ethz.ch/sgc-volumes/sgk-73.pdf

Jäggi, A., R. Dach, O. Montenbruck, U. Hugentobler, H. Bock, G. Beutler (2009): Phase center modeling for LEO GPS receiver antennas and its impact on precise orbit determination. *Journal of Geodesy*, 83(12), 1145-1162, doi: 10.1007/s00190-009-0333-2

Jäggi, A., H. Bock, U. Meyer, G. Beutler, J. van den IJssel (2015): GOCE: assessment of GPS-only gravity field determination. *Journal of Geodesy*, 89(1), 33-48. doi: 10.1007/s00190-014-0759-z

Literature (3)

Jäggi, A., C. Dahle, D. Arnold, H. Bock, U. Meyer, G. Beutler, J. van den IJssel (2016): Swarm kinematic orbits and gravity fields from 18 months of GPS data. *Advances in Space Research*, 57(1), 218-233. doi: 10.1016/j.asr.2015/10.035

Sośnica, K., A. Jäggi, U. Meyer, M. Weigelt, T. van Dam, N. Zehentner, T. Mayer-Gürr (2014): Time varying gravity from SLR and combined SLR and high-low satellite-to-satellite tracking data. GRACE Science Team Meeting 2014, 29th September to 1st October 2014, Potsdam, Germany, available at http://www.bernese.unibe.ch/publist/2014/pres/KS_GRACE-SLR.pdf

Švehla, D., M. Rothacher (2004): Kinematic Precise Orbit Determination for Gravity Field Determination, in *A Window on the Future of Geodesy*, edited by F. Sanso, pp. 181-188, Springer, doi: 10.1007/b139065

Teixeira da Encarnação, J., D. Arnold, A. Bezděk, C. Dahle, E. Doornbos, J. van den IJssel, A. Jäggi, T. Mayer-Gürr, J. Sebera, P. Visser, N. Zehentner (2016): Gravity field models derived from Swarm GPS data. *Earth, Planets and Space*, 68:127. doi: 10.1186/s40623-016-0499-9

van den IJssel, J., J. Encarnação, E. Doornbos, P. Visser (2015): Precise science orbits for the Swarm satellite constellation, *Advances in Space Research*, 56(6), 1042-1055, doi: 10.1016/j.asr.2015.06.002